Hindawi
Shock and Vibration
Volume 2017, Article ID 4018629, 35 pages
https://doi.org/10.1155/2017/4018629

Research Article

Benchmark Solution for Free Vibration of Moderately Thick Functionally Graded Sandwich Sector Plates on Two-Parameter Elastic Foundation with General Boundary Conditions

Haichao Li,[1] Fuzhen Pang,[1] Xueren Wang,[2] and Shuo Li[1]

[1]*College of Shipbuilding Engineering, Harbin Engineering University, Harbin 150001, China*
[2]*Naval Academy of Armament, Beijing 100161, China*

Correspondence should be addressed to Fuzhen Pang; pangfuzhen@hrbeu.edu.cn

Received 2 April 2017; Revised 4 June 2017; Accepted 11 June 2017; Published 12 September 2017

Academic Editor: Lorenzo Dozio

The free vibration analysis of moderately thick functionally graded (FG) sector plates resting on two-parameter elastic foundation with general boundary conditions is presented via Fourier-Ritz method, which is composed of the modified Fourier series approach and the Ritz procedure. The material properties are assumed to vary continuously along the thickness according to the power-law distribution. The bilayered and single-layered functionally graded sector plates are obtained as the special cases of sandwich plates. The first-order shear deformation theory (FSDT) is adopted to construct the theoretical model. Under current framework, regardless of boundary conditions, each displacement and each rotation of plates is represented by the modified Fourier series consisting of a standard Fourier cosine series and several closed-form auxiliary functions introduced to ensure and accelerate the convergence of the series representation. Then, the accurate solutions are obtained by using the Ritz procedure based on the energy function of sector plates. The present method shows good convergence, reliability, and accuracy by comprehensive investigation with some selected classical boundary conditions. Numerous new vibration results for moderately thick FG sandwich sector plates are provided. The effects of the elastic restraint parameters and so forth on free vibration characteristic of sector plates are presented.

1. Introduction

The sector plates have been widespread in many branches of engineering applications such as architectural structures, bridges, hydraulic structures, containers, airplane, missiles, ships, and instruments due to the excellent performance like light weight and an effective form with high load-carrying capacity, economy, and technological effectiveness. As is known to us all, the functionally graded material and the fiber-reinforced composite laminated structures possess outstanding characteristics such as the high specific strength and stiffness, good corrosion resistance, and long fatigue life. Thus, the work of combining the sector plate and composite material is a hot point for a lot of researchers.

In the last years, a large quantity of research efforts has been devoted to the vibration analysis of composite laminated and functionally graded sector plates [1–39] in the literature. In these researches, the scope of the boundary conditions and accuracy of solution for the vibration information of the plate rest on the plate theories and the numerical method. For the moment, the plate theories can be classified into three main categories, namely, the classical plate theory, moderately thick plate theory, and thick plate theory. As is well known, the classical plate theory is the simplest theory constructed from the Kirchhoff hypothesis and only has a few numbers of degrees of freedom in the calculation. Thus, the methods on the basis of the classical plate theory have a high computational efficiency. But, the applied range of the classical plate theory is only limited to the thin plate, and when the plate is relatively thick or when accurate solutions for higher modes of vibration are desired, the results may be unfaithful in practical applications since the classical plate theory neglects the effect of shear and normal deformation in the thickness direction. Thereafter, the moderately thick plate theory including the first-order shear deformation theory and higher-order shear deformation theory is developed which,

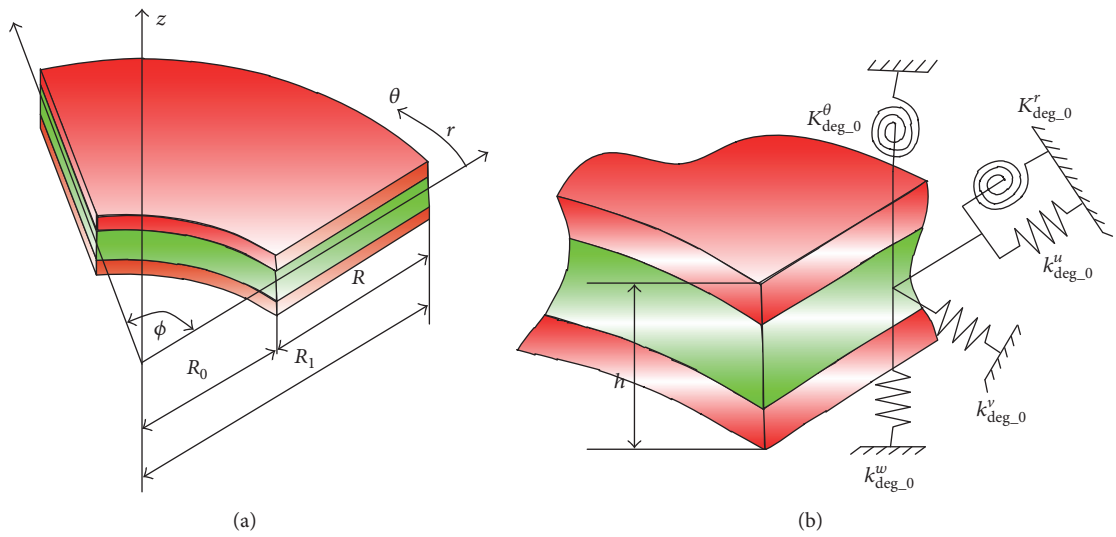

Figure 1: Schematic diagram of FG sandwich annular sector plate: (a) geometry and dimensions of an annular sector plate; (b) partial boundary spring view of the annular sector plate.

respectively, introduce the shear correction factor and the assumption of high-order variations of in-plane displacements taking into account the transverse shear and normal deformation through the plate thickness. Compared with the classical plate theory and moderately thick plate theory, the thick plate theory does not rely on any hypotheses, deserves any numerical precision, and can solve the vibration problem of thick plates. But, it needs more computational resource to obtain the accurate results. Based on the reasonable plate theory, the computational methods of structures have played an important role in the understanding of the structural behaviors. There are many existing methods being applied to the numerical technique to solve the equation of motions and boundary conditions and then obtain the vibration results of the structures, such as differential quadrature method, generalized differential quadrature method, finite element method, and Galerkin's method. In the above methods, when the boundary conditions change, the codes of the solutions need corresponding changes in the calculation process. However, the number of boundary condition in the practical engineering is very large; that is, the boundary conditions of the plate have more than two hundred. Besides, the existing methods are usually good at solving the classical boundary condition, but the boundary conditions of the structures are not always in certain classical case and contain a variety of possible boundary conditions such as elastic restraints in the practical engineering.

Compared with the composite laminated and functionally graded sector plate, the existing results of FG sandwich sector plates are too scarce for engineering applications and comparative studies. However, we can know the importance of the FG sandwich sector plates from the existing published literature about other FG sandwich structures [40–57]. Thus, an accurate frequency and mode shape determination are of considerable importance for the technical design of FG sandwich sector plates. The aim of this paper is to propose a benchmark solution for the vibration characteristics of the FG sandwich sector plates with general boundary conditions and resting on elastic foundation.

In this study, the theoretical model of the FG sandwich sector plate with general boundary conditions and resting on two-parameter elastic foundation is presented. Four common types of sandwich functionally graded sector plates are studied in the study. The material properties are assumed to vary continuously along the thickness according to the power-law distribution. The solution is obtained by using the Fourier-Ritz method, which leads to a generalized eigenvalue problem, and is applied to general boundary conditions of the sector plate. The mathematical fundamentals of the Fourier-Ritz method are discussed in detail in the published literature by Li [58, 59]. It is worthwhile to note that the interest of researches in this procedure is increasing due to its great simplicity and versatility. Therefore, this simple and direct procedure can be applied to a large number of structures, that is, beams [60–63], plates [5, 64–76], shells [77–83], coupled structures [84–88], and so on. In addition, compared with other methods, the present method can obtain accurate results and circumvent the difficulties of programming complex algorithms for the computer as well as the excessive use of storage and computer time.

2. Theoretical Formulations

2.1. Description of the Model. The basic configuration of the problem considered here is an annular sector plate as shown in Figure 1. The geometry and dimensions, namely, the uniform thickness h, inner radius R_0, outer radius R_1, width R ($R = R_1 - R_0$) of plate in the radial direction, and the sector angle ϕ, are defined in a cylindrical coordinate system (r, θ, z). It is noted that the circular sector plate can be viewed as a special case of an annular sector plate whose inner radius is $R_0 = 0$.

It is assumed that the FGM layers of sector plate are made of a mixture of metal and ceramic constituents. The effective material properties of layers vary continuously and smoothly in the thickness direction and are estimated by Voigt's rule. Young's modulus (E), Poisson's ratios (μ), and mass density (ρ) can be expressed as

$$E(z) = (E_c - E_m) V_c(z) + E_m \tag{1a}$$

$$\rho(z) = (\rho_c - \rho_m) V_c(z) + \rho_m \tag{1b}$$

$$\mu(z) = (\mu_c - \mu_m) V_c(z) + \mu_m, \tag{1c}$$

where the subscripts c and m represent the material properties of the ceramic and metal phase, respectively, and $V_c(z)$ is the volume fraction of material constituent M_1. In this paper, to simplify the work, the authors just choose four common types of the sandwich sector plate to investigate, and as shown in Figure 2, two types of moderately thick FG sandwich sector plates are considered in the present study: Type 1: FGM face sheet and homogeneous core; Type 2: homogeneous face sheet and FGM core. The volume fraction $V_c(z)$ of the laminate FGM sector plate is defined as

$$\text{Type 1-1: } \begin{Bmatrix} \left(\dfrac{z - z_1}{z_2 - z_1}\right)^{p^1} & z \in [z_1, z_2] \\ 1 & z \in [z_2, z_3] \\ \left(\dfrac{z - z_4}{z_3 - z_4}\right)^{p^3} & z \in [z_3, z_4] \end{Bmatrix}$$

$$\text{Type 1-2: } \begin{Bmatrix} \left(\dfrac{z - z_2}{z_1 - z_2}\right)^{p^1} & z \in [z_1, z_2] \\ 0 & z \in [z_2, z_3] \\ \left(\dfrac{z - z_3}{z_4 - z_3}\right)^{p^3} & z \in [z_3, z_4] \end{Bmatrix}$$

$$\text{Type 2-1: } \begin{Bmatrix} 1 & z \in [z_1, z_2] \\ \left(\dfrac{z - z_3}{z_2 - z_3}\right)^{p^2} & z \in [z_2, z_3] \\ 0 & z \in [z_3, z_4] \end{Bmatrix} \tag{2}$$

$$\text{Type 2-2: } \begin{Bmatrix} 0 & z \in [z_1, z_2] \\ \left(\dfrac{z - z_2}{z_3 - z_2}\right)^{p^2} & z \in [z_2, z_3] \\ 1 & z \in [z_3, z_4] \end{Bmatrix},$$

where the subscripts p^1, p^2, and p^3 are the power-law exponents used to determine the material profile in FGM. Type 1-1 and Type 1-2 moderately thick FG sandwich sector plates are the sandwich sector plates with FGM face sheets and isotropic core, while Type 2-1 and Type 2-2 moderately thick FG sandwich sector plates are the sandwich sector plates with isotropic face sheets and FGM core. The ratio of thickness of each layer from bottom to top is denoted by the combination of three numbers; for example, "2-2-1" denotes that $h_1 : h_2 : h_3 = 2 : 2 : 1$. It is noted that the single-layered and bilayered FG sector plates can be obtained by setting appropriate ratios of thickness of each layer. To clarify the behavior of (1a), (1b), (1c), and (2), the volume fraction $V_c(z)$ in the thickness direction z for the moderately thick FG sandwich sector plates with various values of power-law index p is shown in Figure 3.

2.2. Energy Expressions. The assumed displacement field for the FG sandwich sector plates based on the first-order shear deformation plate theory can be written as follows:

$$\overline{u}(r, \theta, z, t) = u_0(r, \theta, t) + z\psi_r(r, \theta, t) \tag{3a}$$

$$\overline{v}(r, \theta, z, t) = v_0(r, \theta, t) + z\psi_\theta(r, \theta, t) \tag{3b}$$

$$\overline{w}(r, \theta, z, t) = w_0(r, \theta, t), \tag{3c}$$

where u_0, v_0, and w_0 denote the displacements of the corresponding point on the reference surface in r, θ, and z directions, respectively. ψ_r and ψ_θ are the rotations of the normal to the reference surface about the θ and r direction, respectively, and t is the time. Under the assumption of small deformation and linear strain-displacement relations, the strain components of moderately thick FG sandwich sector plates can be expressed as

$$\begin{aligned} \varepsilon_r &= \varepsilon_r^0 + z\kappa_r, \\ \varepsilon_\theta &= \varepsilon_\theta^0 + z\kappa_\theta \\ \gamma_{r\theta} &= \gamma_{r\theta}^0 + z\kappa_{r\theta}, \end{aligned} \tag{4a}$$

$$\begin{aligned} \gamma_{rz} &= \gamma_{rz}^0, \\ \gamma_{\theta z} &= \gamma_{\theta z}^0, \end{aligned} \tag{4b}$$

where the membrane strains, denoted by ε_r^0, ε_θ^0, $\gamma_{r\theta}^0$, γ_{rz}^0, and $\gamma_{\theta z}^0$, and the curvature changes, denoted by κ_r, κ_θ, and $\kappa_{r\theta}$, of the reference surface are given as

$$\begin{aligned} \varepsilon_r^0 &= \frac{\partial u_0}{\partial r}, \\ \varepsilon_\theta^0 &= \frac{u_0}{r} + \frac{1}{r}\frac{\partial v_0}{\partial \theta}, \\ \gamma_{rz}^0 &= \frac{\partial w}{\partial r} + \psi_r, \\ \gamma_{\theta z}^0 &= \frac{1}{r}\frac{\partial w}{\partial \theta} + \psi_\theta \\ \gamma_{r\theta}^0 &= \frac{\partial v_0}{\partial r} + \frac{1}{r}\frac{\partial u_0}{\partial \theta} - \frac{v_0}{r} \end{aligned} \tag{5a}$$

$$\begin{aligned} \kappa_r &= \frac{\partial \psi_r}{\partial r}, \\ \kappa_\theta &= \frac{1}{r}\frac{\partial \psi_\theta}{\partial \theta} + \frac{\psi_r}{r}, \\ \kappa_{r\theta} &= \frac{\partial \psi_\theta}{\partial r} + \frac{1}{r}\frac{\partial \psi_r}{\partial \theta} - \frac{\psi_\theta}{r}. \end{aligned} \tag{5b}$$

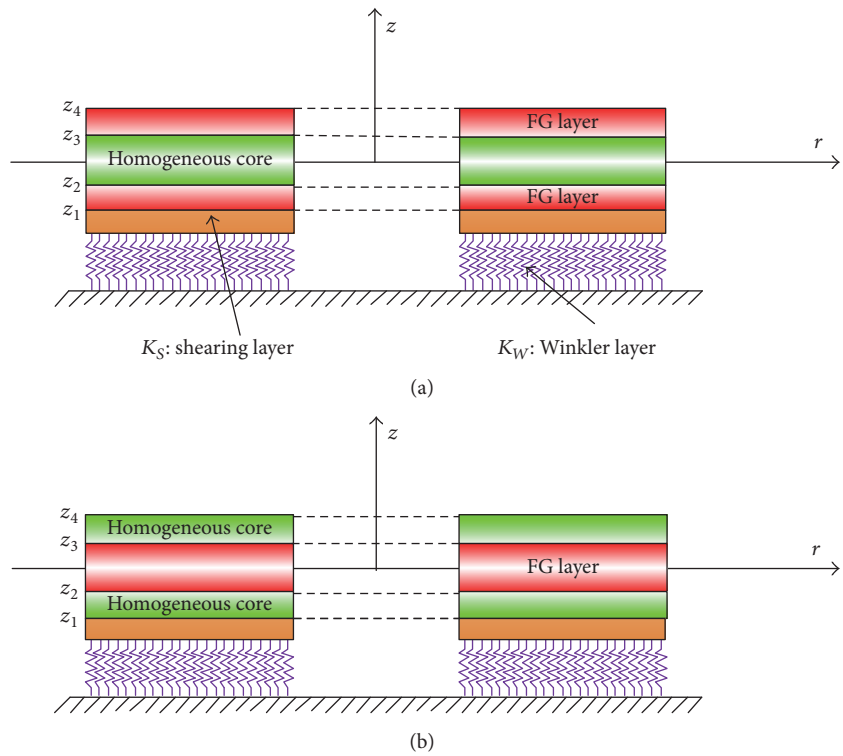

FIGURE 2: The material variation along the thickness of the FG sandwich annular sector plate: (a) FGM face sheet and homogeneous core; (b) homogeneous face sheet and FGM core.

According to Hooke's law, the corresponding stress-strain relations of the eth layer can be written as

$$\begin{Bmatrix} \sigma_r \\ \sigma_\theta \\ \tau_{r\theta} \\ \tau_{rz} \\ \tau_{\theta z} \end{Bmatrix} = \begin{bmatrix} Q_{11}(z) & Q_{12}(z) & 0 & 0 & 0 \\ Q_{12}(z) & Q_{11}(z) & 0 & 0 & 0 \\ 0 & 0 & Q_{66}(z) & 0 & 0 \\ 0 & 0 & 0 & Q_{66}(z) & 0 \\ 0 & 0 & 0 & 0 & Q_{66}(z) \end{bmatrix} \begin{Bmatrix} \varepsilon_r \\ \varepsilon_\theta \\ \gamma_{r\theta} \\ \gamma_{rz} \\ \gamma_{\theta z} \end{Bmatrix}, \tag{6}$$

where the elastic constants Q_{ij} are functions of the thickness coordinate z and are defined as

$$Q_{11}(z) = \frac{E(z)}{1-(\mu(z))^2},$$
$$Q_{12}(z) = \frac{\mu(z)E(z)}{1-(\mu(z))^2}, \tag{7}$$
$$Q_{66}(z) = \frac{E(z)}{2(1+\mu(z))}.$$

By carrying the integration of the stresses over the cross-section, the force and moment resultants can be obtained:

$$\begin{bmatrix} N_r \\ N_\theta \\ N_{r\theta} \\ M_r \\ M_\theta \\ M_{r\theta} \end{bmatrix} = \begin{bmatrix} A_{11} & A_{12} & 0 & B_{11} & B_{12} & 0 \\ A_{12} & A_{11} & 0 & B_{12} & B_{11} & 0 \\ 0 & 0 & A_{66} & 0 & 0 & B_{66} \\ B_{11} & B_{12} & 0 & D_{11} & D_{12} & 0 \\ B_{12} & B_{11} & 0 & D_{12} & D_{11} & 0 \\ 0 & 0 & B_{66} & 0 & 0 & D_{66} \end{bmatrix} \begin{bmatrix} \varepsilon_r^0 \\ \varepsilon_\theta^0 \\ \gamma_{r\theta}^0 \\ \kappa_r \\ \kappa_\theta \\ \kappa_{r\theta} \end{bmatrix} \tag{8}$$

$$\begin{bmatrix} Q_r \\ Q_\theta \end{bmatrix} = \begin{bmatrix} \kappa A_{66} & 0 \\ 0 & \kappa A_{66} \end{bmatrix} \begin{bmatrix} \gamma_{rz}^0 \\ \gamma_{\theta z}^0 \end{bmatrix}, \tag{9}$$

where N_x, N_y, and N_{xy} are the in-plane force resultants, M_x, M_y, and M_{xy} are moment resultants, and Q_x and Q_y are transverse shear force resultants. The shear correction factor κ is computed such that the strain energy due to transverse shear stresses in (9) equals the strain energy due to the true transverse stresses predicted by the three-dimensional elasticity theory. In application, the shear correction factor does not have to be the same in the r and theta direction and depends on many factors such as the geometric and material parameters [89]. However, the aim of this paper is to study the vibration analysis of moderately thick functionally graded sector plates resting on two-parameter elastic foundation with general boundary conditions. Thus, in order to simplify this study and based on existing literature [5, 71], the shear

correction factor κ is selected as a generic parameter $\kappa = 5/6$ in the next calculation. A_{ij}, B_{ij}, and D_{ij} (i, $j = 1$, 2, and 6) are the extensional, extensional-bending coupling, and bending stiffness, and they are, respectively, expressed as

$$\left(A_{ij}, B_{ij}, D_{ij}\right) = \int_{-h/2}^{h/2} Q_{ij}(z)\left(1, z, z^2\right) dz. \tag{10}$$

The strain energy (U_s) of the FG sandwich sector plates during vibration can be defined as

$$\begin{aligned} U_s = \frac{1}{2}\int\int\int_V \left\{N_r\varepsilon_r^0 + N_\theta\varepsilon_\theta^0 + N_{r\theta}\gamma_{r\theta}^0 + M_r\kappa_r + M_\theta\kappa_\theta \right. \\ \left. + M_{r\theta}\kappa_{r\theta} + Q_r\gamma_{rz}^0 + Q_\theta\gamma_{\theta z}^0\right\} r\, dr\, d\theta\, dz. \end{aligned} \tag{11}$$

Substituting (5a), (5b), (8), and (9) into (11), the strain energy expression of the structure can be written in terms of middle plane displacements and rotations.

$$\begin{aligned} U_s = \frac{1}{2}\int_{R_0}^{R_1}\int_0^{\phi}\left\{A_{11}\left(\frac{\partial u_0}{\partial r}\right)^2 + A_{11}\left(\frac{u_0}{r} + \frac{1}{r}\frac{\partial v_0}{\partial \theta}\right)^2 \right. \\ + \kappa A_{66}\left(\frac{\partial w}{\partial r} + \psi_r\right)^2 + A_{66}\left(\frac{\partial v_0}{\partial r} + \frac{1}{r}\frac{\partial u_0}{\partial \theta} - \frac{v_0}{r}\right)^2 \\ + 2A_{12}\left(\frac{\partial u_0}{\partial r}\right)\left(\frac{u_0}{r} + \frac{1}{r}\frac{\partial v_0}{\partial \theta}\right) \\ + \kappa A_{66}\left(\frac{1}{r}\frac{\partial w}{\partial \theta} + \psi_\theta\right)^2 + 2D_{12}\left(\frac{\partial \psi_r}{\partial r}\right) \\ \cdot\left(\frac{1}{r}\frac{\partial \psi_\theta}{\partial \theta} + \frac{\psi_r}{r}\right) + D_{11}\left(\frac{\partial \psi_r}{\partial r}\right)^2 \\ + D_{11}\left(\frac{1}{r}\frac{\partial \psi_\theta}{\partial \theta} + \frac{\psi_r}{r}\right)^2 \\ + D_{66}\left(\frac{\partial \psi_\theta}{\partial r} + \frac{1}{r}\frac{\partial \psi_r}{\partial \theta} - \frac{\psi_\theta}{r}\right)^2 \\ + 2B_{11}\left(\frac{1}{r}\frac{\partial \psi_\theta}{\partial \theta} + \frac{\psi_r}{r}\right)\left(\frac{u_0}{r} + \frac{1}{r}\frac{\partial v_0}{\partial \theta}\right) \\ + 2B_{12}\left(\frac{u_0}{r} + \frac{1}{r}\frac{\partial v_0}{\partial \theta}\right)\left(\frac{\partial \psi_r}{\partial r}\right) + 2B_{11}\left(\frac{\partial \psi_r}{\partial r}\right) \\ \cdot\left(\frac{\partial u_0}{\partial r}\right) + 2B_{12}\left(\frac{1}{r}\frac{\partial \psi_\theta}{\partial \theta} + \frac{\psi_r}{r}\right)\left(\frac{\partial u_0}{\partial r}\right) \\ + 2B_{66}\left(\frac{\partial v_0}{\partial r} + \frac{1}{r}\frac{\partial u_0}{\partial \theta} - \frac{v_0}{r}\right) \\ \left. \cdot\left(\frac{\partial \psi_\theta}{\partial r} + \frac{1}{r}\frac{\partial \psi_r}{\partial \theta} - \frac{\psi_\theta}{r}\right)\right\} r\, dr\, d\theta. \end{aligned} \tag{12}$$

The corresponding kinetic energy (T) function of the FG sandwich sector plate can be given as

$$\begin{aligned} T = \frac{1}{2}\int_{R_0}^{R_0}\int_0^{\theta}\int_{-h/2}^{h/2}\rho\left[\left(\frac{\partial \overline{u}}{\partial t}\right)^2 + \left(\frac{\partial \overline{v}}{\partial t}\right)^2 + \left(\frac{\partial \overline{w}}{\partial t}\right)^2\right] \\ \cdot r\, dr\, d\theta\, dz. \end{aligned} \tag{13}$$

Substituting u, v, and w from (3a), (3b), and (3c) into (13) and performing the integration with respect to z result in

$$\begin{aligned} T = \frac{1}{2}\int_{R_0}^{R_1}\int_0^{\phi}\left\{I_0\left[\left(\frac{\partial u_0}{\partial t}\right)^2 + \left(\frac{\partial v_0}{\partial t}\right)^2 + \left(\frac{\partial w_0}{\partial t}\right)^2\right] \right. \\ + 2I_1\left(\frac{\partial u_0}{\partial t}\right)\left(\frac{\partial \psi_r}{\partial t}\right) + 2I_1\left(\frac{\partial v_0}{\partial t}\right)\left(\frac{\partial \psi_\theta}{\partial t}\right) \\ \left. + I_2\left[\left(\frac{\partial \psi_r}{\partial t}\right)^2 + \left(\frac{\partial \psi_\theta}{\partial t}\right)^2\right]\right\} r\, dr\, d\theta, \end{aligned} \tag{14}$$

where

$$\left(I_0 \;\; I_1 \;\; I_2\right) = \int_{-h/2}^{h/2}\rho(z)\left(1, z^1, z^2\right) dz. \tag{15}$$

Since the main focus of this paper is to develop a unified solution for the vibration analysis of the moderately thick FG sandwich sector plate with general boundary conditions, thus, in order to satisfy the request, the artificial spring boundary technique [90] is adopted here. In this technique, five groups of boundary restraining springs are arranged at all sides of the sector plate to separately simulate the general boundary conditions. Assigning the stiffness of the boundary springs with various values is equivalent to imposing different boundary conditions of the sector plate. For example, the free boundary condition can be readily obtained by setting the spring coefficients to zeros, and the clamped boundary can be obtained by assigning the springs' stiffness to infinity. Thus, the potential energy (U_{sp}) stored in the boundary springs is given as

$$\begin{aligned} U_{\text{sp}} = \frac{1}{2}\int_{-h/2}^{h/2}\int_0^{\phi}\left\{\begin{matrix} R_0\left[k_{r\_0}^u u_0^2 + k_{r\_0}^v v_0^2 + k_{r\_0}^w w^2 + K_{r\_0}^r \psi_r^2 + K_{r\_0}^\theta \psi_\theta^2\right]_{r=R_0} \\ R_1\left[k_{r\_1}^u u_0^2 + k_{r\_1}^v v_0^2 + k_{r\_1}^w w^2 + K_{r\_1}^r \psi_r^2 + K_{r\_1}^\theta \psi_\theta^2\right]_{r=R_1} \end{matrix}\right\} d\theta\, dz + \frac{1}{2} \\ \cdot\int_{-h/2}^{h/2}\int_a^b\left\{\begin{matrix} \left[k_{\text{deg}\_0}^u u_0^2 + k_{\text{deg}\_0}^v v_0^2 + k_{\text{deg}\_0}^w w^2 + K_{\text{deg}\_0}^r \psi_r^2 + K_{\text{deg}\_0}^\theta \psi_\theta^2\right]_{\theta=0} \\ \left[k_{\text{deg}\_1}^u u_0^2 + k_{\text{deg}\_1}^v v_0^2 + k_{\text{deg}\_1}^w w^2 + K_{\text{deg}\_1}^r \psi_r^2 + K_{\text{deg}\_1}^\theta \psi_\theta^2\right]_{\theta=\phi} \end{matrix}\right\} dr\, dz. \end{aligned} \tag{16}$$

As mentioned previously, the main interests of this paper are focused on the moderately thick FG sandwich sector plate which rests on the elastic foundation. As illustrated in Figure 2, the elastic foundation is achieved by applying the two-parameter elastic foundation (Pasternak) mode with Winkler layer (stiffness K_w) and shear layer (stiffness K_s). Therefore, the total energy stored by foundation springs can be given by

$$U_F = \frac{1}{2} \cdot \int_0^{\phi} \int_{R_0}^{R_1} \left(K_w w_0^2 + K_s \left(\frac{\partial w_0}{\partial r} \right)^2 + K_s \left(\frac{1}{r} \frac{\partial w_0}{\partial \theta} \right)^2 \right) \cdot r \, dr \, d\theta. \quad (17)$$

2.3. Equations of Motion. By means of Hamilton's principle, five equilibrium equations of motion of the considered moderately thick FG sandwich sector plate can be obtained, namely,

$$\frac{\partial N_r}{\partial r} + \frac{\partial N_{r\theta}}{r\partial\theta} - \frac{N_\theta}{r} = I_0 \left(\frac{\partial u_0}{\partial t} \right)^2 + I_1 \left(\frac{\partial \psi_r}{\partial t} \right)^2 \quad (18a)$$

$$\frac{\partial N_r}{\partial r} + \frac{\partial N_{r\theta}}{r\partial\theta} - \frac{N_\theta}{r} = I_0 \left(\frac{\partial u_0}{\partial t} \right)^2 + I_1 \left(\frac{\partial \psi_r}{\partial t} \right)^2 \quad (18b)$$

$$\frac{\partial Q_r}{\partial r} + \frac{\partial Q_\theta}{r\partial\theta} = I_0 \left(\frac{\partial w}{\partial t} \right)^2 \quad (18c)$$

$$\frac{\partial M_r}{\partial r} + \frac{\partial M_{r\theta}}{r\partial\theta} - \frac{M_\theta}{r} - Q_r = I_1 \left(\frac{\partial u_0}{\partial t} \right)^2 + I_2 \left(\frac{\partial \psi_r}{\partial t} \right)^2 \quad (18d)$$

$$\frac{\partial M_\theta}{r\partial\theta} + \frac{\partial M_{r\theta}}{\partial r} + \frac{M_{r\theta}}{r} - Q_\theta = I_1 \left(\frac{\partial v_0}{\partial t} \right)^2 + I_2 \left(\frac{\partial \psi_\theta}{\partial t} \right)^2. \quad (18e)$$

Considering (5a) and (5b), (18a), (18b), (18c), (18d), and (18e) show that each displacement and rotation component of the plates at most has second-order derivatives. In next subsection, a set of appropriately constructed admissible displacement functions of the FG sandwich sector plate elements are presented.

2.4. Admissible Displacement Functions and Solution Procedure. The admissible function of the displacement is essential to achieve an accurate and convergent solution in the Ritz procedure. Polynomials and traditional Fourier series are commonly used. However, for the polynomial [91, 92], the lower order polynomials cannot form a complete set, and the higher-order polynomials always tend to become numerically unstable due to the computer round-off errors. And for traditional Fourier series expression, it is only applicable for a few simple boundary conditions and can lead to unavoidable convergence problem for other boundary conditions, which limits the Fourier series to only a few ideal boundary conditions [58]. Take the beam problem, for example, the governing equations for free vibration of a general supported Euler beam are obtained as $D\partial^4 w(x)/\partial x^4 - \rho A\omega^2 w(x) = 0$. From the equation, we can know that the displacement solution $w(x)$ on a beam of length L is required to have up to the fourth derivatives, that is, $w(x) \in C^3$. In general, the displacement function $w(x)$ defined over a domain $[0, L]$ can be expanded into a Fourier series inside the domain excluding the boundary points: $w(x) = \sum_{m=0}^{\infty} A_m \cos(m\pi x/L)$. From the equation, we can see that the displacement function $w(x)$ can be viewed as a part of an even function defined over $[-L, L]$, as shown in Figure 4(a). Thus, the Fourier cosine series is able to correctly converge to $w(x)$ at any point over $[0, L]$. However, its first-derivative $w'(x)$ is an odd function over $[-L, L]$ leading to a jump at end locations. The corresponding Fourier expansion of $w'(x)$ continue on $[0, L]$ and can be differentiated term-by-term only if $w(0) = w(L) = 0$. Thus, its Fourier series expansion (sine series) will accordingly have a convergence problem due to the discontinuity at end points when $w'(x)$ is required to have up to the first-derivative continuity. Recently, Li [58, 59] has proposed an improved Fourier series technique to overcome this problem, and in this technique, a new function $P(x)$ is considered in the displacement function

$$\overline{w}(x) = W(x) + P(x) = \sum_{m=0}^{\infty} A_m \cos\left(\frac{m\pi x}{L} \right) + P(x), \quad (19)$$

where the auxiliary function $P(x)$ in (19) represents an arbitrary continuous function that, regardless of boundary conditions, is always chosen to satisfy the following equations: $P'(0) = w'(0)$, $P'(L) = w'(L)$, $P'''(0) = w'''(0)$, $P'''(L) = w'''(L)$. The actual values of the first and third derivatives (a sine series) at the boundaries need to be determined from the given boundary conditions. Essentially, $\overline{w}(x)$ represents a residual beam function which is continuous over $[0, L]$ and has zero slopes at both ends, as shown in Figure 4(b). Apparently, the cosine series representation of $\overline{w}(x)$ is able to converge correctly to the function itself and its first derivative at every point on the beam. Thus, based on the above analysis, $P(x)$ can be understood as a continuous function which satisfies (19), and its form is not a concern but must be a closed form and sufficiently smooth over a domain $[0, L]$ of the beam to meet the requirements provided by the continuity conditions and boundary constraints. Moreover, it is noticeable that the auxiliary function $P(x)$ can improve the convergent properties of the Fourier series.

According to the above analysis, the displacement field of the moderately thick FG sandwich sector plate can be described by the improved Fourier series technique. The detailed expressions of the displacement and rotation components are given as

$$u_0(r, \theta, t) = U_0(r, \theta) e^{j\omega t} = \left(\sum_{m=0}^{\infty} \sum_{n=0}^{\infty} A_{mn}^u \cos \lambda_{Rm} r \cos \lambda_{\phi n} \theta \right.$$

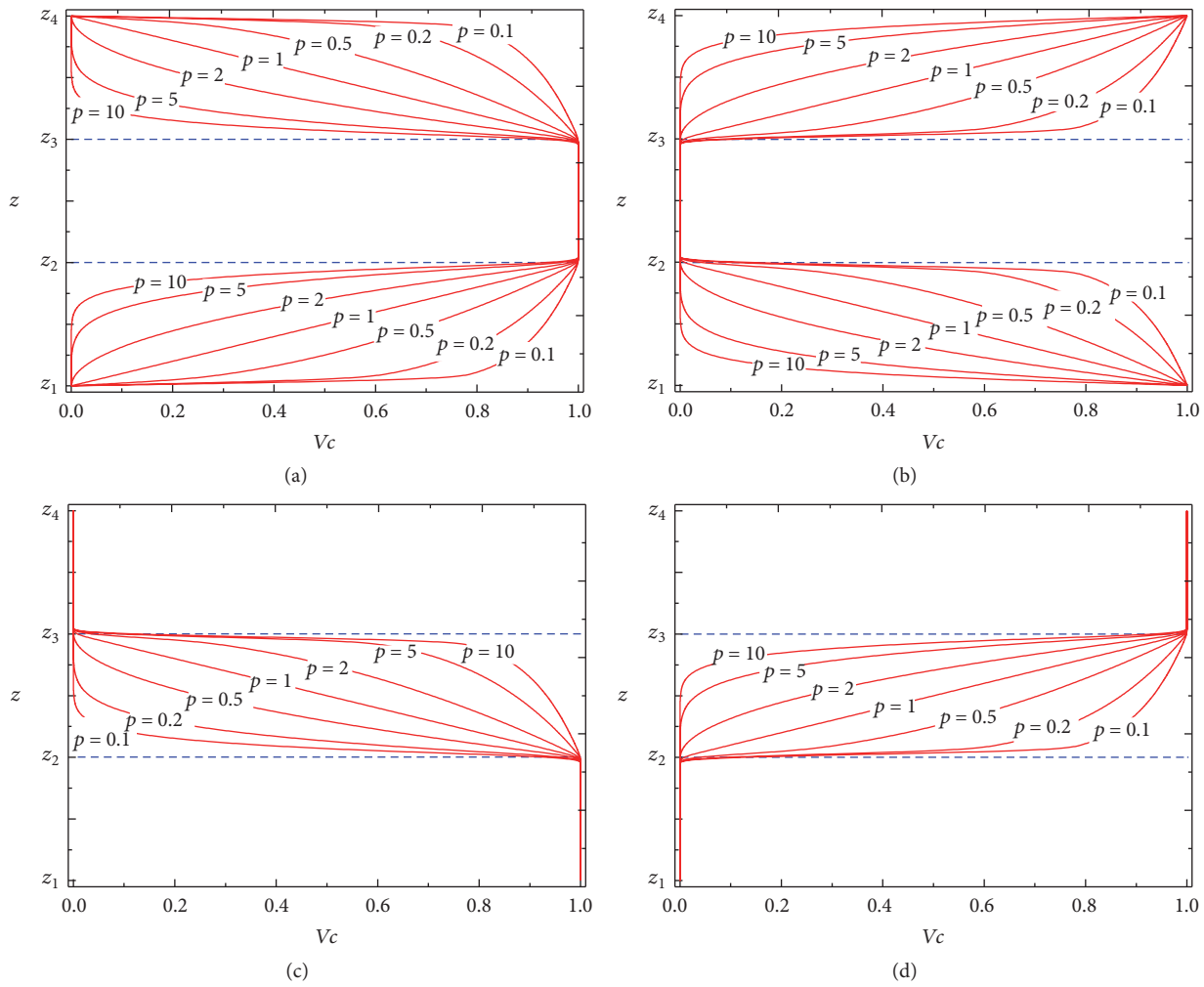

FIGURE 3: Variation of volume fraction Vc along the thickness for different value of power-law exponent: (a) Type 1-1; (b) Type 1-2; (c) Type 2-1; (d) Type 2-2.

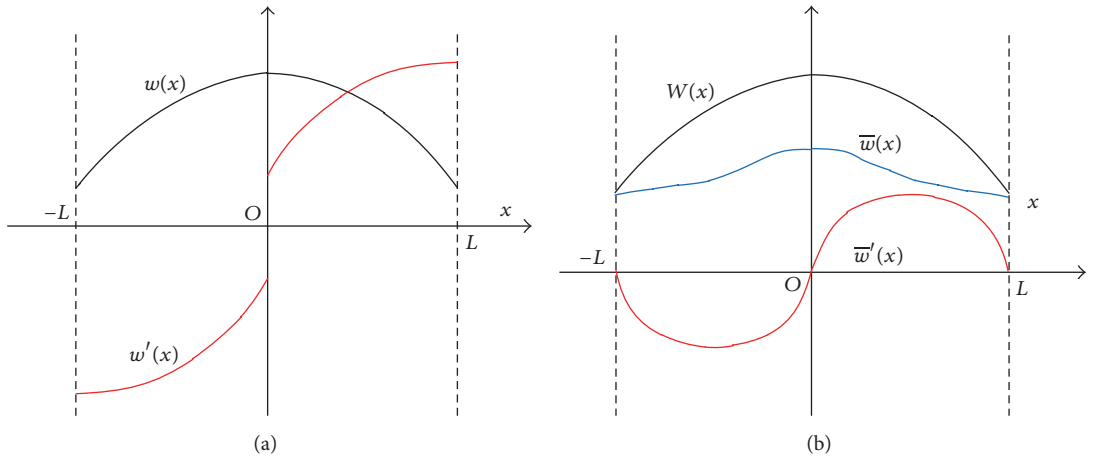

FIGURE 4: An illustration of the possible discontinuities of the displacement at the end points and how they can be equivalently removed mathematically.

$$+\sum_{l=1}^{2}\zeta_b^l(\theta)\sum_{m=0}^{\infty}a_m^l\cos\lambda_{Rm}r+\sum_{l=1}^{2}\zeta_a^l(r)\sum_{n=0}^{\infty}b_n^l\cos\lambda_{\phi n}\theta\Bigg)e^{j\omega t} \tag{20a}$$

$$v_0(r,\theta,t)=V_0(r,\theta)e^{j\omega t}=\Bigg(\sum_{m=0}^{\infty}\sum_{n=0}^{\infty}B_{mn}^{v}\cos\lambda_{Rm}r\cos\lambda_{\phi n}\theta+\sum_{l=1}^{2}\zeta_b^l(\theta)\sum_{m=0}^{\infty}c_m^l\cos\lambda_{Rm}r+\sum_{l=1}^{2}\zeta_a^l(r)\sum_{n=0}^{\infty}d_n^l\cos\lambda_{\phi n}\theta\Bigg)e^{j\omega t} \tag{20b}$$

$$w(r,\theta,t)=W(r,\theta)e^{j\omega t}=\Bigg(\sum_{m=0}^{\infty}\sum_{n=0}^{\infty}C_{mn}^{w}\cos\lambda_{Rm}r\cos\lambda_{\phi n}\theta+\sum_{l=1}^{2}\zeta_b^l(\theta)\sum_{m=0}^{\infty}e_m^l\cos\lambda_{Rm}r+\sum_{l=1}^{2}\zeta_a^l(r)\sum_{n=0}^{\infty}f_n^l\cos\lambda_{\phi n}\theta\Bigg)e^{j\omega t} \tag{20c}$$

$$\psi_r(r,\theta,t)=\psi_r(r,\theta)e^{j\omega t}=\Bigg(\sum_{m=0}^{\infty}\sum_{n=0}^{\infty}D_{mn}^{r}\cos\lambda_{Rm}r\cos\lambda_{\phi n}\theta+\sum_{l=1}^{2}\zeta_b^l(\theta)\sum_{m=0}^{\infty}g_m^l\cos\lambda_{Rm}r+\sum_{l=1}^{2}\zeta_a^l(r)\sum_{n=0}^{\infty}h_n^l\cos\lambda_{\phi n}\theta\Bigg)e^{j\omega t} \tag{20d}$$

$$\psi_\theta(r,\theta,t)=\psi_\theta(r,\theta)e^{j\omega t}=\Bigg(\sum_{m=0}^{\infty}\sum_{n=0}^{\infty}E_{mn}^{\theta}\cos\lambda_{Rm}r\cos\lambda_{\phi n}\theta+\sum_{l=1}^{2}\zeta_b^l(\theta)\sum_{m=0}^{\infty}k_m^l\cos\lambda_{Rm}r+\sum_{l=1}^{2}\zeta_a^l(r)\sum_{n=0}^{\infty}q_n^l\cos\lambda_{\phi n}\theta\Bigg)e^{j\omega t}, \tag{20e}$$

where $\lambda_{Rm}=m\pi/R$, $\lambda_{\phi n}=n\pi/\phi$, and A_{mn}^{u}, B_{mn}^{v}, C_{mn}^{w}, D_{mn}^{r}, and E_{mn}^{θ} are the Fourier coefficients of two-dimensional Fourier series expansions for the displacement functions, respectively. a_m^l, b_n^l, c_m^l, d_n^l, e_m^l, f_n^l, g_m^l, h_n^l, k_m^l, and q_n^l are the supplemented coefficients of the auxiliary functions, where $l=1,2$. ζ_a^l, ζ_b^l, $l=1,2$, represent a set of closed-form sufficiently smooth functions defined over $S:([R_0,R_1]\times[0,\phi])$. In addition, the authors only choose the cosine series as the admissible function of the plate without containing the sine series because compared with the sine series, the cosine series can provide more convergence speed and better accuracy when the plate is with general boundary conditions. More information about the difference between the cosine series and sine series can be seen in [59].

According to the equilibrium equations (18a), (18b), (18c), (18d), and (18e), each of the displacement components at most has two derivatives; thus, it is required that at least two-order derivatives of the admissible functions exist and are continuous at any point on the plate. Therefore two auxiliary functions in r- and θ-direction are supplemented as demonstrated in (20a)–(20e). Such requirements can be readily satisfied by choosing simple auxiliary functions as follows:

$$\zeta_a^1(r)=\frac{R}{2\pi}\sin\left(\frac{\pi\bar{r}}{2R}\right)+\frac{R}{2\pi}\sin\left(\frac{3\pi\bar{r}}{2R}\right),\quad \bar{r}=r-R_0 \tag{21a}$$

$$\zeta_a^2(r)=-\frac{R}{2\pi}\cos\left(\frac{\pi\bar{r}}{2R}\right)+\frac{R}{2\pi}\cos\left(\frac{3\pi\bar{r}}{2R}\right),\quad \bar{r}=r-R_0 \tag{21b}$$

$$\zeta_b^1(\theta)=\frac{\phi}{2\pi}\sin\left(\frac{\pi\theta}{2\phi}\right)+\frac{\phi}{2\pi}\sin\left(\frac{3\pi\theta}{2\phi}\right) \tag{21c}$$

$$\zeta_b^2(\theta)=-\frac{\phi}{2\pi}\cos\left(\frac{\pi\theta}{2\phi}\right)+\frac{\phi}{2\pi}\cos\left(\frac{3\pi\theta}{2\phi}\right). \tag{21d}$$

It is easy to verify that

$$\xi_a^1(R_0)=\xi_a^1(R_1)=\xi_a^{1\prime}(R_1)=0,\quad \xi_a^{1\prime}(R_0)=1 \tag{22a}$$

$$\xi_a^2(R_0)=\xi_a^2(R_1)=\xi_a^{2\prime}(R_0)=0,\quad \xi_a^{2\prime}(R_1)=1 \tag{22b}$$

$$\xi_b^1(0)=\xi_b^1(\phi)=\xi_b^{1\prime}(\phi)=0,\quad \xi_b^{1\prime}(0)=1 \tag{22c}$$

$$\xi_b^1(0)=\xi_b^1(\phi)=\xi_b^{1\prime}(\phi)=0,\quad \xi_b^{1\prime}(0)=1. \tag{22d}$$

The Lagrangian energy function (L) of the moderately thick FG sandwich sector plate can be written as

$$L=T-U_s-U_{\mathrm{sp}}-U_F. \tag{23}$$

Substituting (12), (13), (16), (17), (20a), (20b), (20c), (20d), and (20e) into (23) and performing the Ritz procedure with

respect to each unknown coefficient, the equation of motion for plates can be yielded and is given in the matrix form:

$$\left\{\begin{bmatrix} \mathbf{K}_{uu} & \mathbf{K}_{uv} & \mathbf{0} & \mathbf{K}_{u\psi_r} & \mathbf{K}_{u\psi_\theta} \\ & \mathbf{K}_{vv} & \mathbf{0} & \mathbf{K}_{v\psi_r} & \mathbf{K}_{v\psi_\theta} \\ & & \mathbf{K}_{ww} & \mathbf{K}_{w\psi_r} & \mathbf{K}_{w\psi_\theta} \\ & \text{sym} & & \mathbf{K}_{\psi_r\psi_r} & \mathbf{K}_{\psi_r\psi_\theta} \\ & & & & \mathbf{K}_{\psi_\theta\psi_\theta} \end{bmatrix} - \omega^2 \begin{bmatrix} \mathbf{M}_{uu} & \mathbf{0} & \mathbf{0} & \mathbf{M}_{u\psi_r} & \mathbf{0} \\ & \mathbf{M}_{vv} & \mathbf{0} & \mathbf{0} & \mathbf{M}_{v\psi_\theta} \\ & & \mathbf{M}_{ww} & \mathbf{0} & \mathbf{0} \\ & \text{sym} & & \mathbf{M}_{\psi_r\psi_r} & \mathbf{0} \\ & & & & \mathbf{M}_{\psi_\theta\psi_\theta} \end{bmatrix}\right\} \cdot \begin{Bmatrix} \mathbf{H}_u \\ \mathbf{H}_v \\ \mathbf{H}_w \\ \mathbf{H}_{\psi_r} \\ \mathbf{H}_{\psi_\theta} \end{Bmatrix} = \mathbf{0}, \tag{24}$$

where

$$\mathbf{H}_u = \begin{Bmatrix} A^u_{00}, A^u_{01}, \ldots, A^u_{m'0}, A^u_{m'1}, \ldots, A^u_{m'n'}, \ldots, A^u_{MN}, \\ a^1_0, \ldots, a^1_M, a^2_0, \ldots, a^2_M, b^1_0, \ldots, b^1_N, b^2_0, \ldots, b^2_N \end{Bmatrix} e^{j\omega t} \tag{25a}$$

$$\mathbf{H}_v = \begin{Bmatrix} B^v_{00}, B^v_{01}, \ldots, B^v_{m'0}, B^v_{m'1}, \ldots, B^v_{m'n'}, \ldots, B^v_{MN}, \\ c^1_0, \ldots, c^1_M, c^2_0, \ldots, c^2_M, d^1_0, \ldots, d^1_N, d^2_0, \ldots, d^2_N \end{Bmatrix} e^{j\omega t} \tag{25b}$$

$$\mathbf{H}_w = \begin{Bmatrix} C^w_{00}, C^w_{01}, \ldots, C^w_{m'0}, C^w_{m'1}, \ldots, C^w_{m'n'}, \ldots, C^w_{MN}, \\ e^1_0, \ldots, e^1_M, e^2_0, \ldots, e^2_M, ef^1_0, \ldots, f^1_N, f^2_0, \ldots, f^2_N \end{Bmatrix} e^{j\omega t} \tag{25c}$$

$$\mathbf{H}_{\psi_r} = \begin{Bmatrix} D^r_{00}, D^r_{01}, \ldots, D^r_{m'0}, D^r_{m'1}, \ldots, D^r_{m'n'}, \ldots, D^r_{MN}, \\ g^1_0, \ldots, g^1_M, g^2_0, \ldots, g^2_M, h^1_0, \ldots, h^1_N, h^2_0, \ldots, h^2_N \end{Bmatrix} e^{j\omega t} \tag{25d}$$

$$\mathbf{H}_{\psi_\theta} = \begin{Bmatrix} E^\theta_{00}, E^\theta_{01}, \ldots, E^\theta_{m'0}, E^\theta_{m'1}, \ldots, E^\theta_{m'n'}, \ldots, E^\theta_{MN}, \\ k^1_0, \ldots, k^1_M, k^2_0, \ldots, k^2_M, q^1_0, \ldots, q^1_N, q^2_0, \ldots, q^2_N \end{Bmatrix} e^{j\omega t}. \tag{25e}$$

$\mathbf{K}_{ij}$ and $\mathbf{M}_{ij}$ ($i, j = u, v, w, \psi_x$, and ψ_y) are the submatrices of global stiffness and mass matrices. To clearly clarify the submatrices, the elements of typical matrices $\mathbf{K}_{uu}$ and $\mathbf{M}_{uu}$ are given in the Appendix. By solving (24), the frequencies (or eigenvalues) of moderately thick FG sandwich sector plate can be readily obtained and the mode shapes can be yielded by substituting the corresponding eigenvectors into series representations of displacement and rotation components.

3. Numerical Results and Discussion

In this section, the vibration information of the moderately thick FG sandwich sector plate can be easily obtained by using the MATLAB 7.11.0 to solve (24). Comparison studies and several numerical examples are presented for the verification of the accuracy and applicability of the present method. Take the moderately thick FG sandwich sector plate as the study object; its vibration characteristics under the general boundary conditions including the classical boundary condition, elastic boundary conditions, and their combinations are analyzed. In this paper, authors apply five groups of springs and set them proper stiffness to implement the corresponding boundary conditions as the innovation point. Thus, the first task is to study the boundary spring stiffness. For the sake of brevity, a symbolism is employed to represent the boundary condition of the annular sector plate and circular sector plate; for example, FCSE and CFE denote the annular sector plate with F (free), C (clamped), S (simply supported), and E (elastic restraint) boundary conditions at $r = R_0$, $\theta = 0$, $r = R_1$, and $\theta = \phi$ and the circular sector plate with C, F, and E boundary condition at $\theta = 0$, $r = R_1$, and $\theta = \phi$, respectively. Next, as a power method, the convergence, accuracy, and reliability of the present method should be investigated. Then, the vibration analysis and parameter studies of the moderately thick FG sandwich sector plate without the elastic foundation are presented. The parameter studies contain the power-law exponent, sector angle, material types, and thickness schemes. Lastly, the vibration analysis of the moderately thick FG sandwich sector plate resting on two-parameter foundations with different boundary conditions is conducted and the effects of the elastic foundation coefficients on the free vibration characteristic of the sector plate are presented. In addition, unless otherwise stated, the material constituents M_1 and M_2 are assumed to be alumina and aluminum, respectively. The material properties used in the following analyses are $E_m = 70$ GPa, $\mu_m = 0.3$, $\rho_m = 2707\ \text{kg/m}^3$, $E_c = 380$ GPa, $\mu_c = 0.3$, and $\rho_c = 3800\ \text{kg/m}^3$.

3.1. Determination of the Boundary Spring Stiffness. Figure 5 shows the variations of the lowest three frequency parameters $\Delta\Omega$ of FG sandwich sector plate with respect to the restraint parameters Γ_u, Γ_v, Γ_w, Γ_r, and Γ_θ. The elastic restraint parameters Γ are defined as ratios of the corresponding spring stiffness to the reference bending stiffness $D_m = E_m h^3/12(1-\mu_m{}^2)$; for example, $\Gamma_u = k^u/D_m$, $\Gamma_v = k^v/D_m$, $\Gamma_w = k^w/D_m$, $\Gamma_r = K^r/D_m$, and $\Gamma_\theta = K^\theta/D_m$. Type 1-1, Type 1-2, Type 2-1, and Type 2-2 laminated FGM sector plates are considered in the analysis and the thickness scheme is 2-2-1. The geometric parameters and power-law exponents of the sector plate used are $R_0/R_1 = 0.5$, $\phi = 120^\circ$, $h/R_1 = 0.2$, and $p^1 = p^3 = 5$. The plates under consideration are completely clamped at the circumference boundary condition and free at the boundary $\theta = 0$, while at edge $\theta = \phi$, the plates are elastically supported by only one group of spring components with stiffness varying from $10^{-4}D_m$ to $10^8 D_m$. According to Figure 5, we can see that the change of the boundary elastic restraint parameter Γ has little effect on the frequency

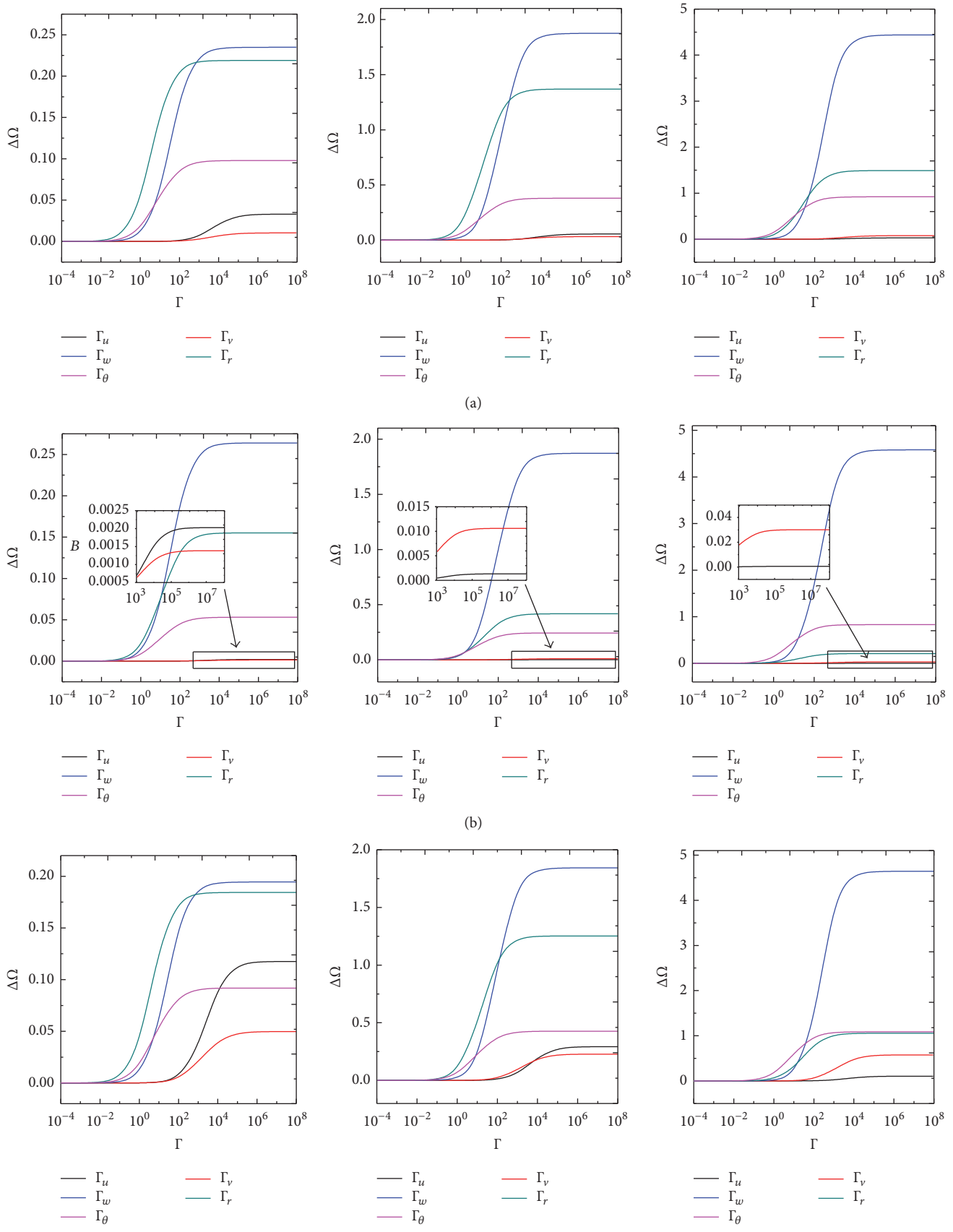

Figure 5: Continued.

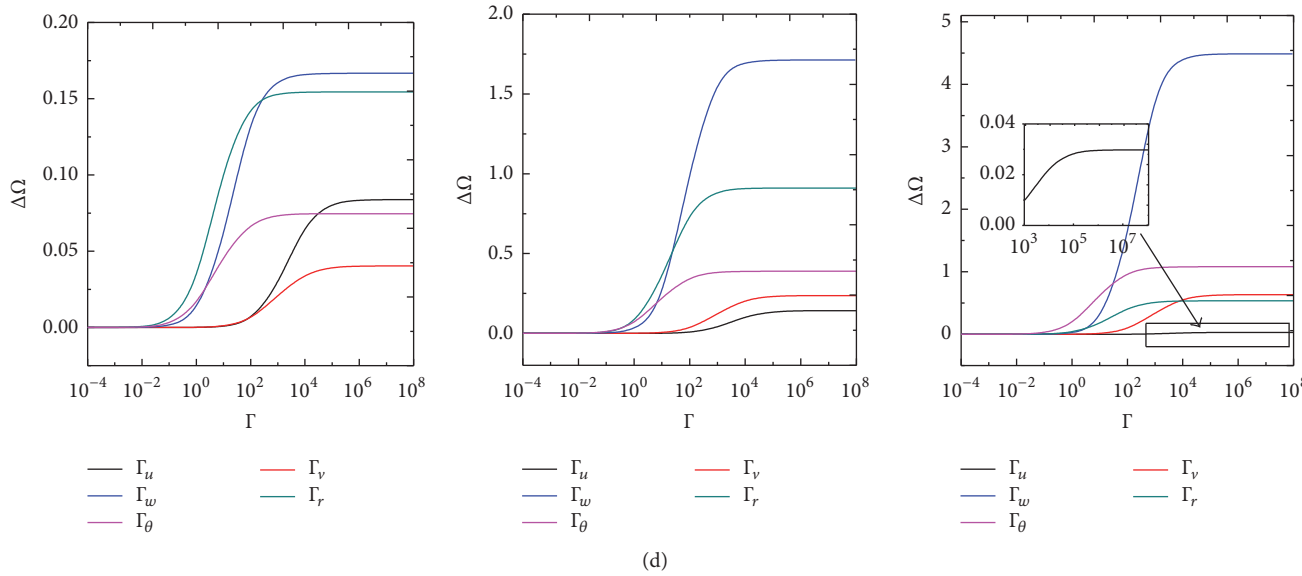

(d)

Figure 5: Variation of the frequency parameters $\Delta\Omega$ versus the elastic restraint parameters Γ for FG sandwich sector plate ($R_0/R_1 = 0.5$, $\phi = 120^\circ$, $h/R_1 = 0.2$, and $p^1 = p^3 = 5$, 2-2-1): (a) Type 1-1; (b) Type 1-2; (c) Type 2-1; (d) Type 2-2.

Table 1: The corresponding elastic restraint parameters for various boundary conditions.

BC	r = constant					θ = constant				
	Γ_u	Γ_v	Γ_w	Γ_r	Γ_θ	Γ_u	Γ_v	Γ_w	Γ_r	Γ_θ
F	0	0	0	0	0	0	0	0	0	0
C	10^8 D	10^8 D	10^8 D	10^8 D	10^8 D	10^8 D	10^8 D	10^8 D	10^8 D	10^8 D
S	0	10^8 D	10^8 D	0	10^8 D	10^8 D	0	10^8 D	10^8 D	0
SD	0	10^8 D	10^8 D	0	0	10^8 D	0	10^8 D	0	0
E^1	10^2 D	10^2 D	10^2 D	10^8 D	10^8 D	10^2 D	10^2 D	10^2 D	10^8 D	10^8 D
E^2	10^8 D	10^8 D	10^8 D	10^2 D	10^2 D	10^8 D	10^8 D	10^8 D	10^2 D	10^2 D
E^3	10^2 D	10^2 D	10^2 D	10^2 D	10^2 D	10^2 D	10^2 D	10^2 D	10^2 D	10^2 D

parameter Ω when it is smaller than $10^{-2}D_m$. However, when it is increased in a certain range, the plate frequencies increase rapidly as the elastic parameters increase, and the frequency parameters approach their utmost and remain unchanged when Γ approaches infinity. It is noted that the certain range is different with respect to different kinds of boundary elastic restraint parameters. The clamped boundary conditions of a plate can be realized by assigning all boundary spring stiffness to 10^8D and the elastic edges can be obtained by setting the stiffness of springs to the proper value. As is well known, the boundary conditions contain a variety of elastic boundary conditions in the practical engineering applications. So, for fear of the overstaffing and unwieldiness, only three kinds of elastic boundary conditions are selected, and the relevant stiffness of the five types of boundary elastic restraint parameters is shown in Table 1.

3.2. Convergence Study. In this subsection, the convergence of the moderately thick FG sandwich sector plate with different boundary conditions is studied. Table 2 shows the convergence of the frequency parameters $\Omega = \omega R_1^2\sqrt{\rho_m h/D_m}$ for completely clamped sector plates. The material type and thickness ratios are taken to be Type 1-1 and 2-2-1, respectively. The geometrical parameters and power-law exponents for the sector plate used in the study are circular sector plate: $\phi = 120^\circ$, $h/R_1 = 0.1$; annular sector plate: $R_0/R_1 = 0.5$, $\phi = 120^\circ$, $h/R_1 = 0.1$; $p^1 = p^3 = 5$. For the fundamental mode, the maximum difference between the $M\times N = 4\times4$ and $M\times N = 18\times18$ is less than 0.162% for the worst case. However, for the higher modes (16th mode), the maximum difference is more than 16.225%. Thus, we can know that using the present method to predict the lower modes merely needs smaller truncation number. It means that the convergence of the present method in the lower modes is faster than that in the higher modes. From the table, we also can know that a highly desired convergence characteristic is observed in that (a) sufficiently accurate results can be obtained with only a small number of terms in the series expansions and (b) the solution is consistently refined as more terms are included in the expansions. However, this should not constitute a problem in practice because one can always verify the accuracy of the solution by increasing the truncation number until a desired numerical precision is achieved. As a matter of fact, this "quality control" scheme can be easily implemented

Table 2: Convergence of frequency parameters Ω for clamped annular sector plate and circular sector plate ($R_0/R_1 = 0.5$, $\phi = 120^\circ$, $h/R_1 = 0.2$, and $p^1 = p^3 = 5$).

$M \times N$	Mode number							
	1	2	3	4	8	10	12	16
Annular sector plate: Type 1-1 (2-2-1)								
4 × 4	93.796	103.03	120.55	187.65	245.38	294.84	351.42	379.08
5 × 5	93.758	102.74	119.84	146.16	238.17	267.17	332.81	376.02
6 × 6	93.680	102.66	119.30	144.14	238.15	266.69	295.52	373.65
7 × 7	93.674	102.60	119.23	143.62	229.48	244.89	294.36	351.15
8 × 8	93.656	102.58	119.10	143.44	229.47	244.72	266.02	351.11
9 × 9	93.655	102.56	119.08	143.29	229.43	244.68	265.83	326.85
10 × 10	93.649	102.55	119.04	143.25	229.42	244.61	265.81	326.66
12 × 12	93.646	102.54	119.00	143.17	229.40	244.56	265.73	326.36
14 × 14	93.645	102.53	118.99	143.14	229.40	244.53	265.69	326.25
16 × 16	93.644	102.53	118.99	143.13	229.39	244.52	265.67	326.19
18 × 18	93.644	102.53	118.99	143.13	229.39	244.51	265.66	326.16
Circular sector plate: Type 1-1 (2-2-1)								
4 × 4	41.679	68.054	91.458	100.58	184.45	221.56	243.92	302.38
5 × 5	41.617	67.665	91.386	99.181	171.33	201.68	221.52	257.70
6 × 6	41.585	67.575	91.114	98.546	169.74	184.82	214.70	249.33
7 × 7	41.574	67.496	91.101	98.424	168.53	184.81	212.39	243.85
8 × 8	41.565	67.477	91.040	98.282	167.86	184.81	208.42	243.85
9 × 9	41.562	67.452	91.037	98.255	167.61	184.81	207.67	243.85
10 × 10	41.559	67.447	91.017	98.208	167.40	184.80	207.22	243.85
12 × 12	41.557	67.435	91.007	98.179	167.24	184.80	206.88	243.84
14 × 14	41.556	67.430	91.003	98.167	167.18	184.80	206.75	243.84
16 × 16	41.555	67.427	91.001	98.160	167.15	184.80	206.69	243.84
18 × 18	41.555	67.426	91.001	98.159	167.15	184.80	206.66	243.84

automatically. In modal analysis, the natural frequencies for higher-order modes tend to converge slower (see Table 1). Thus, an adequate truncation number should be dictated by the desired accuracy of the largest natural frequencies of interest. In view of the excellent numerical behavior of the current solution, the truncation numbers will be simply set as $M = N = 14$ in the following calculations. To further validate the accuracy and reliability of the current method, more numerical examples will be presented. In each case, the convergence study is performed and for brevity purpose, only the converged results are presented.

3.3. Sector Plate with Various Boundary Conditions

3.3.1. Validation and Some New Results. In this subsection, the present method is adopted to analyze the free vibration of moderately thick FG sandwich sector plate with different thickness ratios, power-law exponents, and boundary conditions. Firstly, the validity of the present method for the moderately thick FG sandwich circular sector plate is studied. The comparisons of the frequency parameters $\Omega = \omega R_1^2 \sqrt{\rho_m h/D_m}$ for the FG annular sector plate by the present method and other methods are shown in Table 3. The material type and thickness ratios are taken to be Type 1-1 and 1-0-0, respectively. The geometrical dimensions of the annular sector plates in the analysis are given as $\phi = 45^\circ$, 120°, 240°, and 360°, $h/R = 0.1$ and 0.2, and $R_0/R_1 = 0.5$ and 0.7. The power-law exponents used are $p^1 = p^3 = 0$, 0.5, 1, and 2. Four types of boundary conditions are under consideration in this analysis, that is, SCSC, SSSS, SCSS, and SCSF. The reference results were reported by Saidi et al. [38] using the DQ method on the basis of FSDT. The comparison shows that the current results are in good agreement with those of Saidi et al. [38]. Next, the validity of the present method for the moderately thick FG sandwich circular sector plate is studied. Table 4 shows the first six frequency parameters $\Omega = \omega R_1^2 \sqrt{I_0/(E_c h^3/12(1-\mu_c^2))}$ of FG circular sector plate with different boundary conditions. The material type and thickness ratios are the same as those in Table 3. The geometrical parameters and power-law exponents of the FG circular sector plate are taken to be $h/R_1 = 0.005$ and $p^1 = p^3 = 1$. The results are compared with other published solutions reported by Mirtalaie et al. [39], which use the differential quadrature method based on the Kirchhoff hypothesis. From the table, we can see that there is a good agreement between the present results and the referential data. From Tables 3 and 4, we can learn that the present method has higher accuracy and reliability. In addition, the results of Tables 3 and 4 also show that it is appropriate to define the classical boundary conditions in terms of boundary spring rigidities as in Table 1. Having

Table 3: Comparison of the fundamental frequency Ω for Type 1-1 (1-0-0) annular sector plate with different boundary conditions and some values of p, ϕ, h/R, and R_0/R_1.

ϕ	h/R	R_0/R_1	$p = 0$		$p = 0.5$		$p = 1$		$p = 2$	
			Present	DQM [38]	Present	DQM [38]	Present	DQM [38]	Present	DQM [38]
						SCSC				
45	0.1	0.5	194.8160	194.9900	166.2082	166.3153	150.2243	150.2992	136.4071	136.4535
		0.7	476.2485	476.6814	406.1966	406.4655	367.1207	367.3109	333.4284	333.5481
	0.2	0.5	163.4673	163.6200	141.1496	141.2456	128.2058	128.2741	116.1314	116.1744
		0.7	401.6972	402.0732	347.0488	347.2862	315.3959	315.5654	285.8517	285.9592
						SSSS				
120	0.1	0.5	84.6916	84.7699	71.8487	71.8978	64.7832	64.8181	58.8727	58.8950
		0.7	218.2320	218.4339	185.1097	185.2357	166.8971	166.9869	151.6765	151.7341
	0.2	0.5	80.1166	80.1911	68.2517	68.2982	61.6182	61.6513	55.9117	55.9327
		0.7	170.8277	170.9907	153.3271	153.4349	142.0979	142.1771	128.3715	128.4221
						SCSS				
240	0.1	0.5	113.6641	113.7661	96.6646	96.7273	87.2537	87.2977	79.2726	79.3000
		0.7	318.2095	318.4965	270.5833	270.7604	244.2267	244.3514	221.8914	221.9694
	0.2	0.5	101.6405	101.7348	87.2198	87.2789	79.0084	79.0504	71.6453	71.6718
		0.7	285.3312	285.5963	244.7812	244.9474	221.7106	221.8287	201.0608	201.1356
						SCSF				
360	0.1	0.5	25.4430	25.4653	21.5680	21.5816	19.4433	19.4527	17.6757	17.6815
		0.7	72.2176	72.2815	61.2110	61.2499	55.1774	55.2045	50.1612	50.1778
	0.2	0.5	24.7384	24.7610	21.0203	21.0343	18.9649	18.9748	17.2290	17.2352
		0.7	70.4067	70.4710	59.7989	59.8388	53.9394	53.9677	49.0017	49.0195

Table 4: Comparison of frequency parameters $\Omega = \omega b^2 (I_0/D_c)^{1/2}$ for Type 1-1 (1-0-0) circular sector plate with different boundary conditions and some values of $p = 1$, ϕ, and $h/R_1 = 0.005$.

ϕ	Source of result	Mode number					
		1	2	3	4	5	6
				CCC			
30	DQM [39]	161.6895	257.7845	358.6257	368.9981	496.3537	515.3727
	Present	161.6245	257.6316	358.4922	368.7320	495.9707	515.0906
60	DQM [39]	64.9682	124.6827	127.8239	201.0241	209.1647	215.3604
	Present	64.9699	124.6689	127.8671	200.9819	209.0478	215.2143
				SSS			
30	DQM [39]	85.1070	158.8688	239.4427	248.8392	355.3409	371.3462
	Present	84.1225	157.9932	238.6164	247.5275	354.7307	370.1041
60	DQM [39]	34.6846	81.4720	84.4201	145.3033	152.9561	158.2822
	Present	34.2925	81.1683	84.1225	144.8008	152.4740	157.8930
				SFS			
45	DQM [39]	19.2254	63.5700	70.7899	122.8581	152.5376	156.7239
	Present	19.0321	63.2629	70.7192	122.3353	152.2428	156.3877
90	DQM [39]	4.7166	18.9667	30.4039	41.1333	63.3673	70.7733
	Present	4.6654	18.9548	30.2890	41.0787	63.2629	70.7610
				SCS			
45	DQM [39]	60.1866	120.7868	144.6854	197.7130	242.6680	261.5216
	Present	59.8481	120.3583	144.5406	197.1593	242.4294	261.2852
90	DQM [39]	30.0711	59.9173	72.8029	98.2194	120.4645	132.3217
	Present	29.9584	59.8491	72.6442	98.1400	120.3593	132.0831

confidence in the current method, more numerical examples will be presented in the later examples.

In the Introduction, we mention that the results of the moderately thick FG sandwich sector plate are very scarce in the published literature. Therefore, in the next examples, the authors will give some new results for the moderately thick FG sandwich sector plate with various boundary conditions to support the predesign in practical engineering applications. Tables 5–8 show the fundamental frequency parameter $\Omega = \omega R_1^2 \sqrt{\rho_m h/D_m}$ for moderately thick FG sandwich annular sector plate with different boundary conditions including the classical case, elastic restraint, and their combination. Five kinds of thickness ratios, that is, 1-0-1, 1-1-1, 2-2-1, 1-2-1, and 1-8-1, are taken be in the analysis. The power-law exponents of the FG circular sector plate are used as $p^1 = p^3 = p = 0.5$, 5, and 20. The geometrical dimensions of the annular sector plates in the analysis are given as $R_0/R_1 = 0.5$, $h/R_1 = 0.2$, and the sector angle $\phi = 120^\circ$, 60°, 240°, and 350° corresponding to Tables 5–8, respectively. Also, Tables 9–12 show the fundamental frequency parameter $\Omega = \omega R_1^2 \sqrt{\rho_m h/D_m}$ for the moderately thick FG sandwich circular sector plate subject to various boundary conditions. The geometrical and material parameter are the same as Tables 5–8 expect for $R_0 = 0$. From Tables 5–12, it is evident that the fundamental frequency parameters are quite sensitive to the change of the power-law exponents and boundary conditions. For the case of classical boundary conditions, the increase of the power-law exponent leads to the decrease of the fundamental frequency parameters of sector plates. However, when the sector plate is under the elastic boundary condition, the effects of the power-law exponent on the fundamental frequencies of the sector plate are different and a little more complex. For the sector plate with the conditions of $E^1E^1E^1E^1$ and $E^3E^3E^3E^3$, the fundamental frequencies increase as the power-law exponent increases. While the boundary condition of the sector plate is $E^2E^2E^2E^2$, the variation of the frequencies for the sector plate is similar to the classical boundary conditions'. In addition, the thickness ratio and material type have significant influence on the fundamental frequencies of the sector plate regardless of the boundary conditions and power-law exponents. Some mode shapes for moderately thick FG sandwich sector plates with different boundary conditions and geometric and material parameters are depicted in Figures 6 and 7.

3.3.2. Parameter Studies. The effects of power-law exponents, sector angles, material types, and thickness schemes with different boundary conditions are investigated in this subsection. Figure 8 shows the variations of fundamental frequency parameter $\Omega = \omega R_1^2 \sqrt{\rho_m h/D_m}$ of Type 1 annular sector plate against different power-law exponents p^1 and p^3. The geometric dimensions used for the analysis are $R_0/R_1 = 0.5$, $\phi = 120^\circ$, and $h/R_1 = 0.2$. The scope of the power-law exponents p^1 and p^3 is from 0 to 10 and the interval of power-law exponents is equal to 0.5. The thickness ratio of the annular sector plate is taken to be 1-2-1. The classical boundary condition (CCCC), classical-elastic boundary condition ($CE^1E^1E^1$), and the elastic boundary condition ($E^3E^3E^3E^3$) are considered in this analysis. Also, the variations of the fundamental frequency parameter $\Omega = \omega R_1^2 \sqrt{\rho_m h/D_m}$ of Type 1 circular sector plate versus the power-law exponents p^1 and p^3 are shown in Figure 9. The geometric dimensions, thickness ratios, and material parameters are the same as those in Figure 8 expect for $R_0 = 0$. Three types of boundary conditions, that is, CCC, CE^1E^1, and $E^3E^3E^3$, are selected in this analysis. From the figures, we can see that when the sector plate is under classical and classical-elastic boundary conditions, the frequency parameters Ω decrease monotonically as the power-law exponents p^1 and p^3 increase irrespective of the shape and material type of plates. When all edges of the sector plate are under the E^3 elastic boundary condition, the variations of the fundamental frequency parameters turn more complex. For Type 1 annular sector plate with the $E^3E^3E^3E^3$ boundary condition, the frequency parameters Ω increase monotonically as the power-law exponents p^1 and p^3 increase. For circular sector plate under $E^3E^3E^3$, when the material type is Type 1-1, the variation rule of the fundamental frequency parameters are the same as the classical boundary condition. However, when the material type is Type 1-2, the variations of the fundamental frequency parameters firstly increase and then decrease as the power-law exponents p^1 and p^3 increase. Next, the variations of the fundamental frequencies of Type 2 sector plate with different boundary conditions and power-law exponent p^2 are shown in Figure 10. The geometric dimensions and material parameters are the same as those in Figures 8 and 9. The thickness ratio of the sector plate adopts 2-2-1 in this analysis. From the figure, we can see that the variation of fundamental frequencies of the sector plate decreases or increases as the power-law exponent p^2 increases regardless of the material type, when the sector plate is under the all clamped and elastic boundary conditions. For the annular sector plate with the condition $CE^1E^1E^1$, the fundamental frequencies decrease monotonically versus the increase of the power-law exponent p^2 irrespective of the material type. However, for the case of circular sector plate, the variations of fundamental frequencies between the materials of Type 2-1 and Type 2-2 are different. For Type 2-1, the fundamental frequencies monotonically decrease with the power-law exponent p^2 increasing. For Type 2-2, the fundamental frequencies firstly decrease and then slow up.

From Tables 5–12, we can see that the variations of fundamental frequency parameter Ω of the sector plate subjected to classical case, elastic restraints, and classical-elastic restraints with different material types, power-law exponents, and sector angles are more complex. Thus, in the following examples, the authors will fully illustrate the effects of the boundary conditions and material type on vibration characteristics of the sector plates with different sector angles. Figures 11 and 12 show the variations of fundamental frequency parameter Ω of annular sector plate and circular sector plate with different sector angles, material types, and boundary conditions, respectively. The geometric dimensions are the same as Figure 10 and the power-law exponent is $p^1 = p^2 = p^3 = 5$. From the figures, it is obvious

Table 5: Fundamental frequency parameter Ω for Type 1-1 annular sector plate with various boundary conditions ($R_0/R_1 = 0.5$, $h/R_1 = 0.2$, $p^1 = p^3 = p$, and $\phi = 120^\circ$).

Scheme	p	Boundary conditions								
		CCCC	CSDCSD	CFCF	SSSS	$CE^1E^1E^1$	E^2SE^2S	$E^1E^1E^1E^1$	$E^2E^2E^2E^2$	$E^3E^3E^3E^3$
1-0-1	0.5	83.742	82.842	81.118	55.349	34.047	77.251	19.655	77.934	19.545
	5	57.995	57.391	56.216	36.938	28.436	55.623	20.461	56.131	20.360
	20	52.505	51.933	50.852	35.162	27.747	50.698	20.557	51.178	20.462
1-1-1	0.5	87.605	86.661	84.854	58.112	34.924	80.210	19.393	80.911	19.284
	5	68.130	67.450	66.062	41.725	29.797	64.338	19.966	64.903	19.857
	20	64.141	63.505	62.199	39.006	29.012	60.936	20.079	61.470	19.972
2-2-1	0.5	88.644	87.685	85.855	59.033	35.226	81.021	19.345	81.727	19.236
	5	71.264	70.549	69.100	45.066	30.500	66.988	19.886	67.583	19.777
	20	67.600	66.928	65.555	43.306	29.726	63.908	19.999	64.476	19.891
1-2-1	0.5	89.857	88.883	87.024	59.994	35.536	81.935	19.268	82.645	19.160
	5	74.871	74.112	72.585	46.578	31.236	69.935	19.723	70.550	19.614
	20	71.362	70.648	69.192	43.815	30.395	67.028	19.815	67.615	19.706
1-8-1	0.5	94.455	93.414	91.443	64.301	36.964	85.462	19.044	86.188	18.944
	5	88.816	87.863	86.032	58.664	35.090	81.072	19.253	81.776	19.145
	20	87.424	86.492	84.694	57.332	34.652	79.981	19.300	80.678	19.191

Table 6: Fundamental frequency parameter Ω for Type 1-2 annular sector plate with various boundary conditions ($R_0/R_1 = 0.5$, $h/R_1 = 0.2$, $p^1 = p^3 = p$, and $\phi = 60^\circ$).

Scheme	p	Boundary conditions								
		CCCC	CSDCSD	CFCF	SSSS	$CE^1E^1E^1$	E^2SE^2S	$E^1E^1E^1E^1$	$E^2E^2E^2E^2$	$E^3E^3E^3E^3$
1-0-1	0.5	102.850	95.998	87.258	78.574	38.733	91.343	22.240	95.758	22.163
	5	76.806	71.963	65.038	60.777	34.563	70.427	23.721	74.004	23.636
	20	64.244	60.045	54.466	49.650	31.736	59.240	23.789	62.580	23.703
1-1-1	0.5	94.916	88.841	80.407	74.595	37.235	85.537	22.951	89.569	22.871
	5	71.671	67.123	60.701	56.482	33.443	65.929	23.804	69.388	23.718
	20	62.000	57.896	52.590	47.469	31.205	57.188	23.750	60.497	23.664
2-2-1	0.5	92.094	86.160	78.038	72.068	36.881	83.145	23.083	87.211	23.002
	5	70.286	65.781	59.549	55.071	33.105	64.653	23.805	68.127	23.720
	20	61.477	57.391	52.155	46.926	31.077	56.702	23.737	60.009	23.652
1-2-1	0.5	89.217	83.617	75.535	70.882	36.331	81.015	23.298	84.838	23.216
	5	68.690	64.293	58.193	53.831	32.770	63.268	23.818	66.672	23.732
	20	60.784	56.729	51.574	46.262	30.914	56.071	23.722	59.363	23.636
1-8-1	0.5	74.201	69.559	62.817	58.962	34.055	68.220	23.787	71.684	23.702
	5	62.252	58.139	52.800	47.727	31.266	57.420	23.756	60.731	23.670
	20	58.386	54.429	49.575	47.727	30.333	53.861	23.649	57.119	23.564

that the frequency parameters Ω change monotonically as the sector angle ϕ increases regardless of the boundary condition and material type. For the circular sector plate, the frequency parameters Ω decrease monotonically as the sector angle ϕ increases irrespective of the type of the boundary condition and material. For the case of CCC, CFC, and CE^1E^1, when the sector angle is in the region of 5° to 70°, the frequency parameters Ω of plate rapidly decrease as the sector angle increases. While the sector angle is beyond this region, the frequency parameters firstly slow down and then remain unchanged when the sector angle reaches a critical value. But, for the $E^3E^3E^3$ boundary condition, the frequency parameters always decrease with the increase of the sector angle ϕ in the whole region. Also, the variations of frequency parameters Ω for the annular sector plate with CCCC, CFCF, and $CE^1E^1E^1$ are similar to the circular sector plate with CCC, CFC, and CE^1E^1. However, for the case of $E^3E^3E^3E^3$ annular sector plate, the frequency parameters Ω firstly rapidly increase and then remain unchanged as the sector angle ϕ increases irrespective of the material type.

Lastly, the authors will investigate the effect of material types and thickness schemes on vibration characteristics of the moderately thick FG sandwich sector plate. Figures 13 and 14, respectively, show the variations of fundamental

Table 7: Fundamental frequency parameter Ω for Type 2-1 annular sector plate with various boundary conditions ($R_0/R_1 = 0.5$, $h/R_1 = 0.2$, $p^1 = p^3 = p$, and $\phi = 240^\circ$).

Scheme	p	Boundary conditions								
		CCCC	CSDCSD	CFCF	SSSS	$CE^1E^1E^1$	E^2SE^2S	$E^1E^1E^1E^1$	$E^2E^2E^2E^2$	$E^3E^3E^3E^3$
0-1-1	0.5	68.585	68.501	68.095	35.473	30.189	65.252	18.993	65.111	18.894
	5	57.232	57.154	56.819	27.694	28.656	55.339	19.421	55.201	19.333
	20	51.863	51.794	51.485	25.214	27.396	50.437	19.349	50.309	19.267
1-1-1	0.5	75.442	75.355	74.899	40.403	31.030	70.824	18.495	70.659	18.390
	5	70.101	70.017	69.597	36.811	30.281	66.526	18.861	66.388	18.761
	20	69.015	68.931	68.520	35.845	30.216	65.635	18.955	65.499	18.856
2-2-1	0.5	80.246	80.151	79.669	42.453	32.156	74.609	18.278	74.417	18.170
	5	72.233	72.149	71.713	38.569	30.463	68.252	18.680	68.104	18.578
	20	70.785	70.701	70.275	37.509	30.290	67.079	18.787	66.938	18.686
1-2-1	0.5	77.281	77.191	76.727	40.949	31.549	72.308	18.454	72.131	18.348
	5	68.712	68.627	68.221	35.452	30.246	65.384	18.997	65.248	18.898
	20	66.897	66.812	66.421	33.868	30.136	63.863	19.135	63.730	19.038
1-8-1	0.5	81.224	81.125	80.641	41.890	32.816	75.469	18.390	75.266	18.281
	5	65.437	65.352	64.973	32.732	30.000	62.600	19.223	62.463	19.127
	20	61.124	61.040	60.688	29.688	29.473	58.836	19.396	58.698	19.304

Table 8: Fundamental frequency parameter Ω for Type 2-2 annular sector plate with various boundary conditions ($R_0/R_1 = 0.5$, $h/R_1 = 0.2$, $p^1 = p^3 = p$, and $\phi = 350^\circ$).

Scheme	p	Boundary conditions								
		CCCC	CSDCSD	CFCF	SSSS	$CE^1E^1E^1$	E^2SE^2S	$E^1E^1E^1E^1$	$E^2E^2E^2E^2$	$E^3E^3E^3E^3$
0-1-1	0.5	88.492	88.459	88.180	43.936	34.434	80.910	17.573	80.937	17.470
	5	75.956	75.929	75.677	39.875	30.844	71.202	18.046	71.227	17.952
	20	73.509	73.483	73.235	38.734	30.337	69.250	18.167	69.275	18.075
1-1-1	0.5	75.223	75.197	74.946	39.359	30.759	70.633	18.110	70.659	18.017
	5	69.903	69.878	69.642	35.863	30.034	66.362	18.485	66.388	18.396
	20	68.819	68.794	68.563	34.922	29.974	65.474	18.580	65.499	18.492
2-2-1	0.5	72.482	72.456	72.214	37.588	30.375	68.454	18.311	68.479	18.220
	5	66.472	66.446	66.231	32.806	29.890	63.505	18.780	63.531	18.694
	20	64.791	64.765	64.561	31.458	29.771	62.068	18.888	62.093	18.804
1-2-1	0.5	77.052	77.025	76.773	39.890	31.273	72.105	18.066	72.131	17.971
	5	68.515	68.489	68.262	34.539	30.006	65.222	18.622	65.248	18.534
	20	66.702	66.676	66.460	32.995	29.904	63.704	18.763	63.730	18.677
1-8-1	0.5	80.972	80.942	80.685	40.804	32.530	75.240	17.995	75.266	17.897
	5	65.240	65.214	65.008	31.888	29.774	62.438	18.854	62.463	18.769
	20	60.927	60.902	60.716	28.921	29.262	58.674	19.039	58.698	18.957

frequency parameter Ω for the annular sector plate and circular sector plate with different material types and thickness schemes. The geometric dimensions and power-law exponent are the same as Figures 11 and 12. For Type 1-1 sector plate with compete clamped boundary conditions, the fundamental frequency parameters decrease as the thickness of layer increases except for 1-n-1 thickness schemes. On the contrary, the fundamental frequency parameters increase as the thickness of layer increases except for 1-n-1 thickness schemes while the boundary condition of sector plate is completely elastic boundary conditions (annular sector plate: $E^3E^3E^3E^3$; circular sector plate: $E^3E^3E^3$). For Type 1-2 circular sector plates, the fundamental frequency parameters decrease as the thickness of layer increases irrespectively of the boundary condition. However, for the annular sector plate, the variation is different and a little more complex. For the case of the CCCC boundary condition with n-1-1 and 1-1-n thickness schemes, the fundamental frequency parameters increase as the thickness of layer increases. And for the plate with 1-n-1 thickness schemes, the fundamental frequency parameters decrease as the thickness of layer increases. As to the case of the $E^3E^3E^3E^3$ boundary condition, the increase of thickness of layer leads to the decrease of fundamental frequency parameters regardless of the thickness schemes. For Type 2 sector plate with completely clamped boundary condition, the fundamental frequency parameters decrease

Table 9: Fundamental frequency parameter Ω for Type 1-1 circular sector plate with various boundary conditions ($h/R_1 = 0.2$, $p^2 = p$, and $\phi = 120^\circ$).

Scheme	p	Boundary conditions								
		CCC	CSDC	CFC	SSS	CE^1E^1	E^2SE^2	$E^1E^1E^1$	$E^2E^2E^2$	$E^3E^3E^3$
1-0-1	0.5	44.469	35.027	11.934	27.121	20.578	33.940	16.508	41.593	16.347
	5	30.024	23.414	7.849	17.890	18.659	23.195	16.508	29.195	16.363
	20	28.149	22.255	7.637	17.323	18.372	22.108	16.451	27.491	16.315
1-1-1	0.5	46.635	36.771	12.549	28.509	20.755	35.468	16.338	43.277	16.178
	5	34.280	26.468	8.724	19.955	19.113	26.042	16.396	32.954	16.240
	20	32.115	24.754	8.139	18.622	18.801	24.429	16.355	31.040	16.202
2-2-1	0.5	47.319	37.352	12.773	29.005	20.836	35.982	16.311	43.815	16.152
	5	36.114	27.952	9.251	21.140	19.373	27.426	16.425	34.560	16.266
	20	34.053	26.301	8.677	19.836	19.097	25.883	16.412	32.764	16.256
1-2-1	0.5	48.050	37.956	12.996	29.503	20.905	36.508	16.261	44.370	16.102
	5	38.089	29.524	9.790	22.372	19.591	28.880	16.376	36.236	16.217
	20	35.966	27.787	9.166	20.966	19.301	27.267	16.361	34.412	16.203
1-8-1	0.5	51.195	40.668	14.066	31.858	21.294	38.879	16.129	46.770	15.972
	5	47.136	37.121	12.641	28.733	20.742	35.754	16.232	43.632	16.073
	20	46.164	36.284	12.313	28.009	20.613	35.008	16.253	42.864	16.093

Table 10: Fundamental frequency parameter Ω for Type 1-2 circular sector plate with various boundary conditions ($h/R_1 = 0.2$, $p^2 = p$, and $\phi = 60^\circ$).

Scheme	p	Boundary conditions								
		CCC	CSDC	CFC	SSS	CE^1E^1	E^2SE^2	$E^1E^1E^1$	$E^2E^2E^2$	$E^3E^3E^3$
1-0-1	0.5	83.200	73.456	40.445	60.463	32.862	70.464	20.773	77.188	20.663
	5	62.649	55.874	31.352	47.089	29.586	54.879	21.972	60.223	21.858
	20	52.107	46.162	25.564	38.308	27.380	45.696	21.864	50.698	21.752
1-1-1	0.5	77.305	68.797	38.470	57.830	32.230	66.602	21.397	72.678	21.285
	5	58.402	52.026	29.124	43.810	28.742	51.273	21.991	56.435	21.877
	20	50.174	44.333	24.428	36.538	26.941	43.941	21.785	48.911	21.675
2-2-1	0.5	74.936	66.600	37.159	55.808	31.740	64.596	21.502	70.726	21.389
	5	57.199	50.864	28.387	42.649	28.467	50.157	21.972	55.348	21.859
	20	49.715	43.889	24.145	36.093	26.832	43.512	21.762	48.485	21.653
1-2-1	0.5	72.846	65.036	36.585	54.502	31.548	63.294	21.685	69.030	21.572
	5	55.899	49.717	27.745	41.689	28.216	49.087	21.963	54.170	21.850
	20	49.119	43.328	23.799	35.556	26.696	42.975	21.733	47.931	21.624
1-8-1	0.5	60.581	54.097	30.426	45.333	29.232	53.231	22.008	58.397	21.894
	5	50.394	44.544	24.562	36.749	26.992	44.144	21.795	49.116	21.685
	20	47.025	41.327	22.539	33.583	26.201	41.044	21.612	45.978	21.504

as the thickness of layer increases except for Type 2-1 n-1-1 and Type 2-2 1-1-n thickness schemes. The change rule of the fundamental frequency parameters on the sector plate with elastic boundary conditions reverses in contrast to the clamped boundary condition. In addition, it also can be easily seen that according to Figures 13 and 14, for Type 1 material distribution, the results of the 1-1-n and n-1-1 thickness schemes are coincident in the same material type. For Type 2 material distribution, the results of Type 2-1 and Type 2-2 are coincident in the same thickness schemes.

Based on the above analysis, the vibration characteristics of the moderately thick FG sandwich sector plate strongly depend on the material type, thickness schemes, power-law exponent, and boundary conditions.

3.4. Sector Plate Resting on Two-Parameter Elastic Foundations. In the practical engineering, the structures are usually laid on a soil medium and the vibration analysis of these structures with such elastic foundation and general boundary conditions is necessary and of great significance. In this subsection, the first goal is to check the accuracy of the present method on the vibration analysis of the moderately thick FG sandwich sector plate resting on elastic foundations. The comparison of frequency parameters Ω for Type 1-1

Table 11: Fundamental frequency parameter Ω for Type 2-1 circular sector plate with various boundary conditions ($h/R_1 = 0.2$, $p^2 = p$, and $\phi = 240^\circ$).

Scheme	p	Boundary conditions								
		CCC	CSDC	CFC	SSS	CE^1E^1	E^2SE^2	$E^1E^1E^1$	$E^2E^2E^2$	$E^3E^3E^3$
0-1-1	0.5	25.799	18.485	4.253	15.269	15.798	18.158	13.669	24.736	13.476
	5	22.950	16.821	3.988	14.151	15.387	16.626	13.585	22.239	13.418
	20	20.700	15.152	3.579	12.728	14.766	15.023	13.159	20.178	13.011
1-1-1	0.5	27.614	19.630	4.461	16.114	15.861	19.195	13.535	26.235	13.329
	5	26.055	18.597	4.259	15.318	15.782	18.252	13.615	24.949	13.419
	20	25.876	18.517	4.257	15.284	15.796	18.184	13.656	24.805	13.462
2-2-1	0.5	29.629	21.124	4.812	17.374	16.063	20.571	13.556	27.892	13.343
	5	26.508	18.852	4.292	15.483	15.770	18.478	13.548	25.316	13.348
	20	26.127	18.610	4.249	15.304	15.758	18.259	13.576	25.001	13.379
1-2-1	0.5	28.507	20.314	4.628	16.704	15.984	19.833	13.585	26.985	13.376
	5	25.901	18.567	4.278	15.345	15.821	18.235	13.685	24.832	13.492
	20	25.631	18.468	4.288	15.328	15.837	18.155	13.746	24.612	13.555
1-8-1	0.5	30.612	21.966	5.047	18.155	16.274	21.365	13.698	28.729	13.483
	5	25.350	18.338	4.278	15.267	15.823	18.042	13.770	24.370	13.582
	20	24.398	17.841	4.225	14.987	15.706	17.593	13.773	23.543	13.594

Table 12: Fundamental frequency parameter Ω for Type 2-2 circular sector plate with various boundary conditions ($h/R_1 = 0.2$, $p^2 = p$, and $\phi = 350^\circ$).

Scheme	p	Boundary conditions								
		CCC	CSDC	CFC	SSS	CE^1E^1	E^2SE^2	$E^1E^1E^1$	$E^2E^2E^2$	$E^3E^3E^3$
0-1-1	0.5	29.907	20.840	4.640	19.172	15.254	20.389	12.621	27.916	12.377
	5	24.600	16.933	3.734	15.548	14.713	16.692	12.413	23.527	12.190
	20	23.758	16.341	3.604	15.003	14.621	16.128	12.371	22.804	12.155
1-1-1	0.5	24.421	16.819	3.712	15.444	14.711	16.585	12.427	23.377	12.206
	5	23.029	15.914	3.530	14.622	14.616	15.729	12.446	22.189	12.238
	20	22.861	15.832	3.520	14.553	14.619	15.654	12.476	22.046	12.270
2-2-1	0.5	23.685	16.337	3.613	15.005	14.669	16.130	12.443	22.752	12.228
	5	22.589	15.745	3.523	14.493	14.632	15.577	12.552	21.814	12.352
	20	22.348	15.646	3.516	14.419	14.613	15.486	12.581	21.601	12.385
1-2-1	0.5	25.197	17.390	3.843	15.972	14.819	17.130	12.496	24.043	12.270
	5	22.877	15.866	3.532	14.588	14.637	15.688	12.503	22.062	12.298
	20	22.622	15.759	3.525	14.503	14.633	15.589	12.548	21.843	12.347
1-8-1	0.5	27.025	18.761	4.166	17.247	15.066	18.437	12.648	25.592	12.414
	5	22.364	15.631	3.505	14.397	14.606	15.468	12.560	21.611	12.363
	20	21.505	15.171	3.431	14.012	14.456	15.032	12.535	20.841	12.348

(1-0-0) annular sector plates on Winkler foundations with various boundary conditions is shown in Table 13. The results obtained from the ABAQUS based on FEA method are tabulated in the table for comparison due to the lack of the reference data of the published literature. The geometry parameters of the annular sector plates are given as $R_0/R_1 = 0.5$, $\phi = 90^\circ$, and $h/R_1 = 0.2$. For general purpose, the nondimensional foundation parameters are used in this analysis: $K_W = K_w \times {R_1}^4/D_m$ and $K_S = K_s \times {R_1}^2/D_m$. Two kinds of Winkler foundation stiffness K_W, that is, 10 and 100, are taken in this analysis. From the table, a consistent agreement of present results and referential data is clear. The discrepancy is very small and does not exceed 1% for the worst case. In addition, the table shows that the increasing of Winkler foundation stiffness contributes to the increase of frequencies of the sector plate.

What has been mentioned above is the results of vibration characteristics for the moderately thick FG sandwich sector plate resting on two-parameter elastic foundation, which is limited in the published literature. Thus, the author will

Table 13: Comparison of frequency parameters Ω for Type 1-1 (1-0-0) annular sector plates on Winkler foundations with various boundary conditions ($R_0/R_1 = 0.5$, $\phi = 90^\circ$, $h/R_1 = 0.2$, and $p_1 = p_3 = 0$).

(KW, KG)	Mode number	CCCC			FFFF			CSCS		
		Present	FEM	Error (%)	Present	FEM	Error (%)	Present	FEM	Error (%)
(10, 0)	1	101.04	101.61	0.56	27.05	27.24	0.70	98.73	99.29	0.57
	2	119.56	120.17	0.51	37.04	37.25	0.56	113.70	114.26	0.49
	3	148.92	149.68	0.51	50.79	50.81	0.03	128.81	129.06	0.19
	4	154.35	154.56	0.14	58.99	59.17	0.31	141.92	142.58	0.47
	5	184.85	185.88	0.55	77.94	78.16	0.28	152.79	153.00	0.14
	6	196.96	198.36	0.71	87.03	87.05	0.03	178.77	179.68	0.51
(100, 0)	1	101.56	102.55	0.97	28.74	28.91	0.59	99.25	100.25	0.99
	2	119.99	120.95	0.79	38.28	38.58	0.77	114.14	115.07	0.80
	3	149.25	150.29	0.69	50.79	50.81	0.03	128.81	129.06	0.19
	4	154.35	154.56	0.14	59.75	60.18	0.72	142.27	143.21	0.66
	5	185.12	186.35	0.66	78.52	78.73	0.28	152.79	153.00	0.14
	6	197.21	198.82	0.81	87.03	87.05	0.03	179.04	180.17	0.62

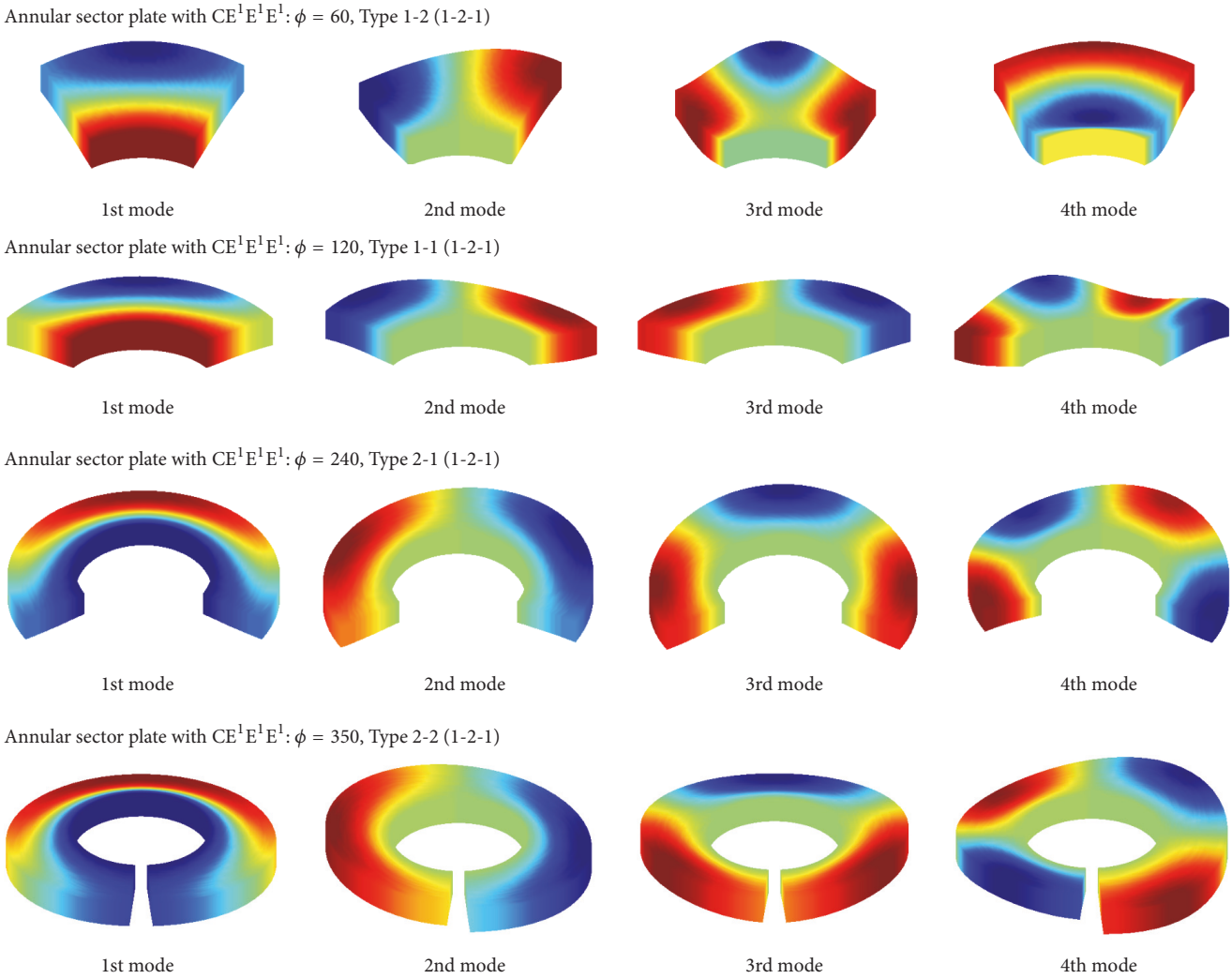

Figure 6: Mode shapes of the FG sandwich annular sector plate with $CE^1E^1E^1$ boundary condition and different sector angles.

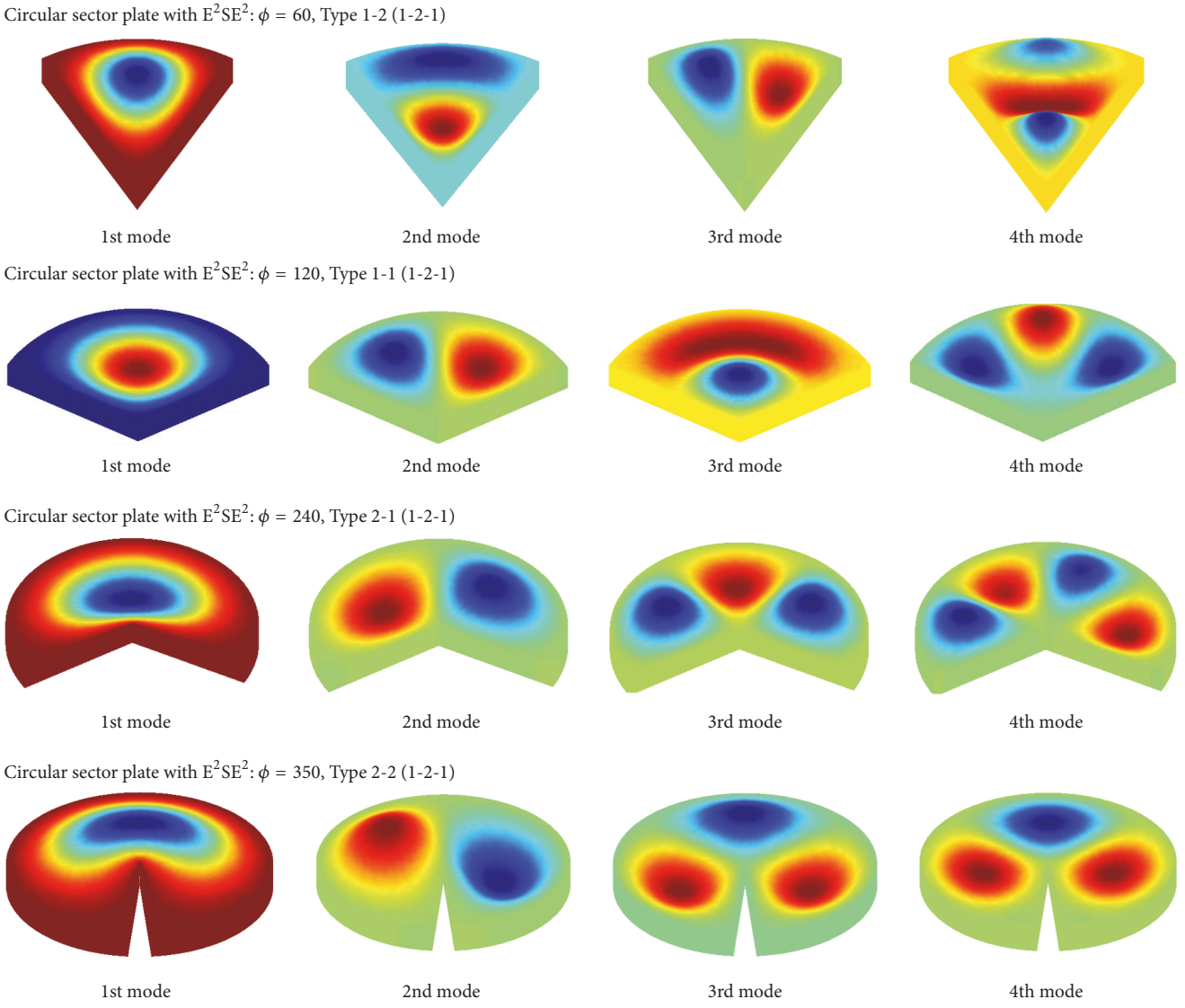

Figure 7: Mode shapes of the FG sandwich circular sector plate with E^2SE^2 boundary condition and different sector angles.

present some new results of moderately thick FG sandwich sector plates resting on two-parameter elastic foundation with various boundary conditions, material types, and foundation coefficients using the present method in the next examples. These results can be as the benchmark solutions for future computational methods in this field. The fundamental frequency parameter Ω for the annular sector plate and circular sector plate with different boundary conditions, material types, and elastic foundation coefficients are shown in Tables 14 and 15, respectively. From the tables, it is clear that the variation of the coefficients has the significant effect on frequency parameters of the sector plate. In order to further study the influence of foundation coefficients on vibration characteristics of the moderately thick FG sandwich sector plate, the variations of the fundamental frequency parameters Ω versus the Winkler foundation stiffness and shearing layer stiffness for annular sector plate and circular sector plate are presented in Figures 15 and 16, respectively. It can be easily obtained that regardless of the boundary conditions, material type, and shape of the plate, there exists a certain range of the elastic foundation coefficients during which the frequency parameter Ω increases and out of which the influence on frequency parameter Ω can be neglected.

4. Conclusions

In the present study, the vibration characteristics of the moderately thick FG sandwich sector plate are investigated. The annular sector plate and circular sector plate with four common types of material distributions, thickness schemes, classical and elastic boundary conditions, and various geometry constants are incorporated. The first-order shear deformation plate theory is employed to include the effects of rotary inertias and shear deformation. The energy expression of the plate is expressed as a function of five displacement components by using the kinematic and constitutive relations.

Table 14: Fundamental frequency parameter Ω for annular sector plate with various boundary conditions and material types ($R_0/R_1 = 0.5$, $\phi = 120^\circ$, $h/R_1 = 0.2$, and $p^1 = p^2 = p^3 = p$).

(KW, KG)	p	Boundary conditions								
		CCCC	CSDCSD	CFCF	CSCS	CE^1CE^1	E^2SE^2S	$E^1E^1E^1E^1$	$E^2E^2E^2E^2$	$E^3E^3E^3E^3$
Type 1-1 (2-2-1)										
(10, 10)	0.5	90.522	89.567	87.632	89.674	89.042	83.012	19.380	83.713	19.380
	5	73.835	73.120	71.544	73.192	72.946	69.642	20.166	70.235	20.090
	20	70.370	69.699	68.191	69.764	69.563	66.756	20.320	67.323	20.234
(10, 100)	0.5	105.518	104.589	101.772	104.683	103.066	98.766	19.380	99.425	19.380
	5	93.191	92.491	89.841	92.546	91.158	89.502	20.173	90.074	20.173
	20	90.876	90.217	87.584	90.265	88.880	87.711	20.366	88.263	20.365
(100, 100)	0.5	105.831	104.904	102.099	104.997	103.389	99.097	19.380	99.755	19.380
	5	93.576	92.878	90.243	92.933	91.555	89.899	20.173	90.471	20.173
	20	91.280	90.622	88.005	90.669	89.296	88.125	20.366	88.677	20.365
Type 1-2 (2-2-1)										
(10, 10)	0.5	83.227	82.291	80.354	82.397	81.477	78.022	20.444	78.694	20.444
	5	65.098	64.393	62.809	64.472	63.873	62.579	21.186	63.134	21.186
	20	57.950	57.345	55.941	57.413	57.003	56.131	21.266	56.626	21.193
(10, 100)	0.5	101.277	100.373	97.371	100.460	98.366	96.747	20.444	97.387	20.444
	5	85.865	85.396	74.553	85.411	75.644	85.318	21.187	85.839	21.187
	20	77.059	76.696	66.901	76.701	68.098	76.697	21.305	77.056	21.305
(100, 100)	0.5	101.652	100.749	97.521	100.835	98.441	97.135	20.444	97.775	20.444
	5	85.865	85.404	74.554	85.420	75.644	85.348	21.187	85.839	21.187
	20	77.059	76.697	66.901	76.701	68.098	76.697	21.305	77.056	21.305
Type 2-1 (2-2-1)										
(10, 10)	0.5	84.174	83.314	81.544	83.387	82.961	78.145	19.719	78.850	19.717
	5	76.294	75.520	73.953	75.564	75.310	71.886	20.230	72.581	20.219
	20	74.898	74.130	72.599	74.169	73.931	70.757	20.352	71.454	20.340
(10, 100)	0.5	100.681	99.821	97.138	99.874	98.445	95.280	19.722	95.986	19.721
	5	95.109	94.256	91.774	94.272	93.031	91.124	20.247	91.929	20.243
	20	94.226	93.337	90.916	93.346	92.149	90.445	20.372	91.302	20.368
(100, 100)	0.5	101.020	100.161	97.492	100.214	98.795	95.633	19.722	96.339	19.721
	5	95.488	94.632	92.171	94.647	93.424	91.510	20.247	92.319	20.244
	20	94.614	93.720	91.322	93.728	92.551	90.838	20.372	91.701	20.369
Type 2-2 (2-2-1)										
(10, 10)	0.5	76.761	75.979	74.394	76.026	75.745	72.279	20.234	72.973	20.225
	5	71.047	70.274	68.805	70.313	70.024	67.595	20.748	68.291	20.739
	20	69.482	68.713	67.255	68.753	68.435	66.274	20.868	66.960	20.860
(10, 100)	0.5	95.506	94.654	92.140	94.673	93.389	91.466	20.248	92.258	20.246
	5	92.119	90.905	85.329	90.907	87.243	88.700	20.771	89.851	20.767
	20	91.249	89.712	82.231	89.730	83.971	87.816	20.891	89.202	20.888
(100, 100)	0.5	95.884	95.030	92.536	95.048	93.780	91.853	20.249	92.647	20.246
	5	92.538	91.287	85.389	91.291	87.279	88.822	20.771	90.280	20.768
	20	91.681	90.057	82.264	90.083	83.990	88.194	20.891	89.642	20.888

Table 15: Fundamental frequency parameter Ω for circular sector plate with various boundary conditions and material types ($\phi = 120^\circ$, $h/R_1 = 0.2$, and $p^1 = p^2 = p^3 = p$).

(KW, KG)	p	Boundary conditions								
		CCC	CSDSD	CFC	CSC	CE^1E^1	E^2CE^2	$E^1E^1E^1$	$E^2E^2E^2$	$E^3E^3E^3$
						Type 1-1 (2-2-1)				
(10, 10)	0.5	49.067	35.093	15.397	39.729	21.501	47.290	16.598	45.630	16.459
	5	38.629	27.661	12.888	31.189	20.261	37.845	16.857	37.116	16.730
	20	36.774	26.473	12.541	29.772	20.058	36.126	16.902	35.522	16.779
(10, 100)	0.5	61.880	50.832	27.164	54.445	25.231	60.311	16.695	58.832	16.695
	5	55.308	47.427	26.216	49.943	24.801	54.623	17.346	53.978	17.345
	20	54.348	47.099	26.161	49.404	24.815	53.783	17.497	53.251	17.497
(100, 100)	0.5	62.411	51.467	28.366	55.040	26.536	60.855	16.695	59.388	16.695
	5	55.956	48.171	27.583	50.652	26.194	55.279	17.346	54.642	17.345
	20	55.023	47.866	27.563	50.135	25.911	54.465	17.497	53.939	17.497
						Type 1-2 (2-2-1)				
(10, 10)	0.5	48.273	36.215	16.399	40.329	22.268	46.823	17.555	45.444	17.418
	5	38.187	28.868	14.075	32.353	21.065	37.571	17.809	36.981	17.690
	20	33.685	25.898	12.888	28.601	20.241	33.299	17.566	32.930	17.463
(10, 100)	0.5	62.582	53.284	28.603	55.930	25.792	61.359	17.557	60.189	17.557
	5	56.710	50.599	27.835	42.896	23.948	56.230	18.029	55.767	18.029
	20	54.211	49.201	27.309	38.461	23.213	53.919	18.035	53.637	18.035
(100, 100)	0.5	63.184	53.975	29.902	56.093	25.792	61.972	17.557	60.813	17.557
	5	57.452	51.410	29.325	42.897	23.948	56.978	18.029	56.520	18.029
	20	55.007	50.058	28.869	38.461	23.213	54.719	18.035	54.440	18.035
						Type 2-1 (2-2-1)				
(10, 10)	0.5	45.085	32.207	14.401	36.416	21.073	43.762	16.779	42.542	16.642
	5	40.914	29.476	13.586	33.169	20.750	40.008	17.073	39.180	16.942
	20	40.378	29.203	13.540	32.813	20.753	39.528	17.161	38.750	17.031
(10, 100)	0.5	59.248	49.411	26.795	52.533	25.079	58.090	16.980	57.014	16.978
	5	56.875	48.481	26.700	50.992	25.156	56.102	17.404	55.392	17.400
	20	56.666	48.513	26.774	50.873	25.238	55.946	17.501	55.286	17.497
(100, 100)	0.5	59.822	50.085	28.061	53.168	26.444	58.675	16.980	57.610	16.978
	5	57.508	49.246	28.050	51.662	26.029	56.744	17.404	56.042	17.400
	20	57.311	49.205	28.141	51.536	25.828	56.599	17.501	55.947	17.497
						Type 2-2 (2-2-1)				
(10, 10)	0.5	41.276	29.759	13.690	33.489	20.813	40.343	17.091	39.489	16.959
	5	39.492	29.102	13.702	32.507	20.919	38.751	17.486	38.066	17.359
	20	39.075	29.014	13.745	32.337	20.949	38.375	17.578	37.723	17.454
(10, 100)	0.5	57.144	48.672	26.770	51.223	25.198	56.347	17.405	55.613	17.402
	5	56.671	49.199	27.215	49.839	25.074	56.066	17.792	55.505	17.788
	20	56.603	49.076	27.346	48.227	24.789	56.038	17.870	55.513	17.867
(100, 100)	0.5	57.775	49.395	28.117	51.893	26.033	56.987	17.405	56.262	17.402
	5	57.354	49.956	28.631	50.040	25.076	56.756	17.793	56.202	17.789
	20	57.300	49.096	28.780	48.295	24.791	56.742	17.871	56.224	17.867

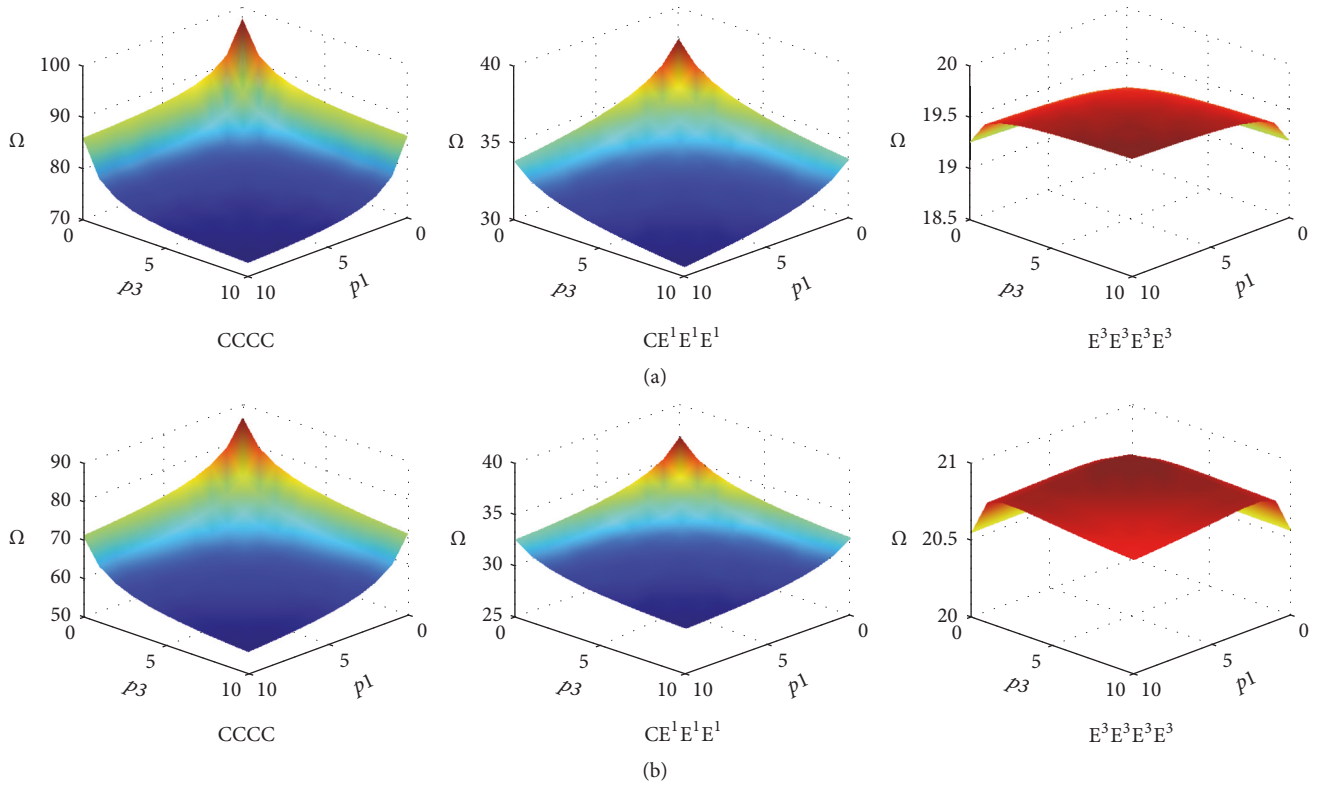

FIGURE 8: Variations of fundamental frequency parameter Ω of Type 1 annular sector plate against different power-law exponents: (a) Type 1-1 (1-2-1); (b) Type 1-2 (1-2-1).

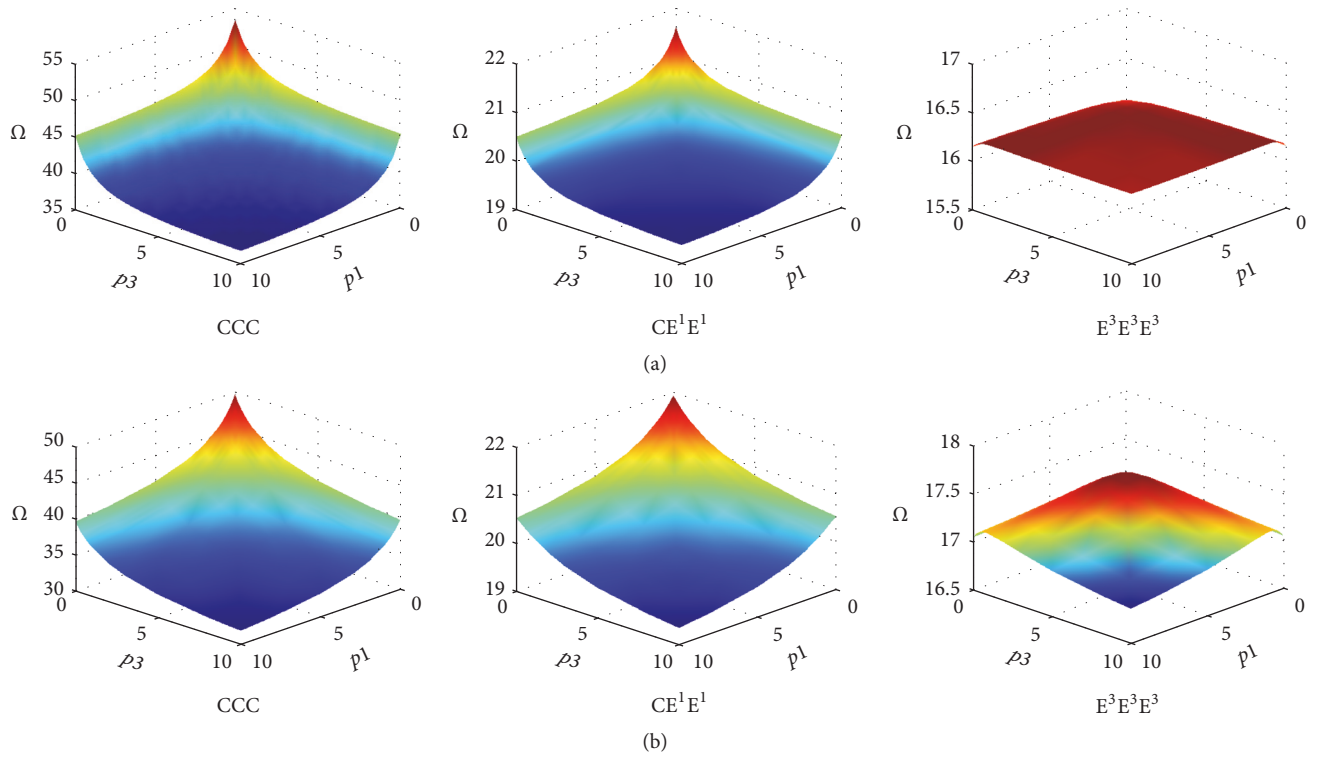

FIGURE 9: Variations of fundamental frequency parameter Ω of Type 1 circular sector plate against different power-law exponents: (a) Type 1-1 (1-2-1); (b) Type 1-2 (1-2-1).

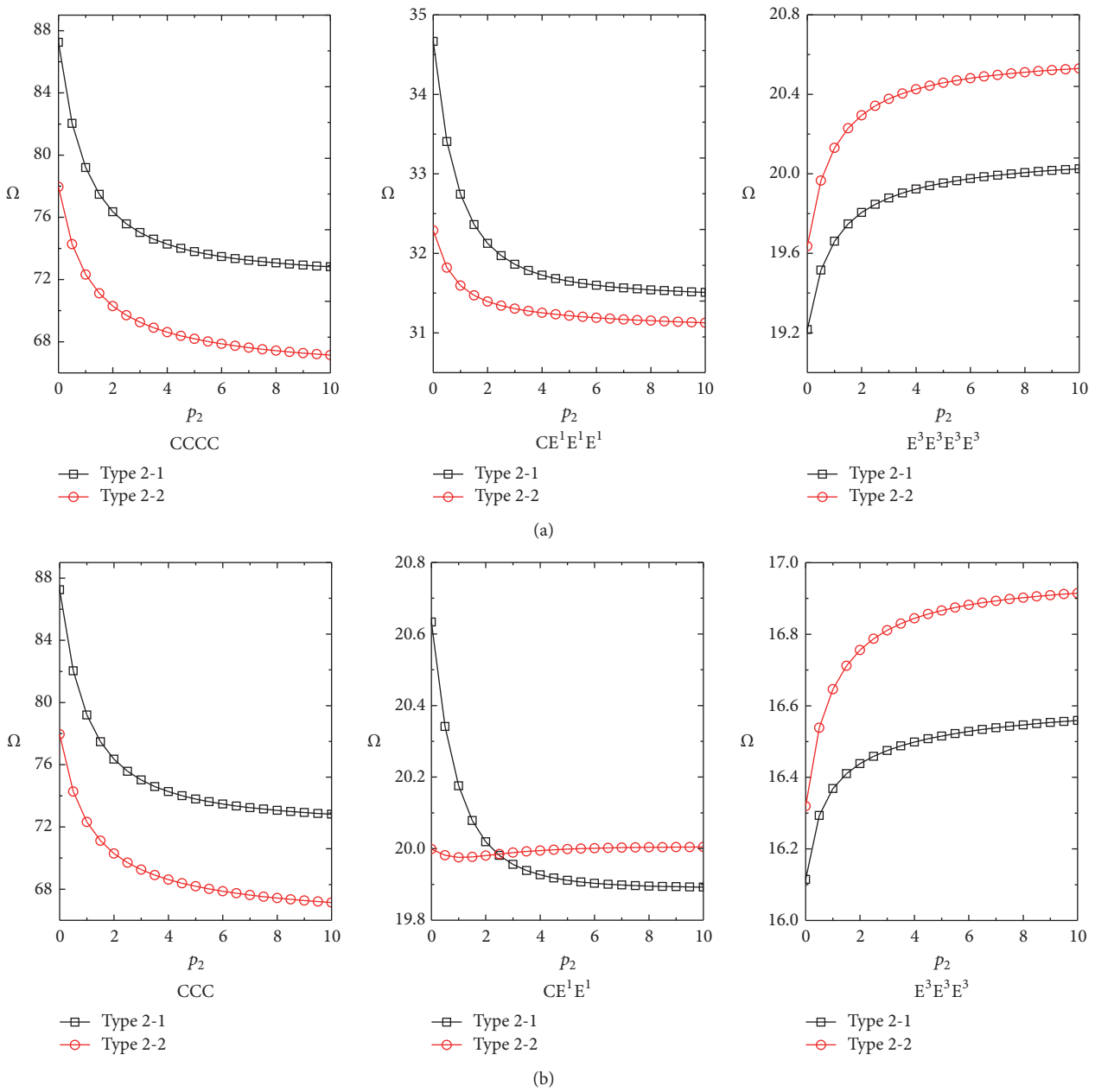

FIGURE 10: Variations of fundamental frequency parameter Ω of Type 2 (2-2-1) sector plate against different power-law exponents: (a) annular sector plate; (b) circular sector plate.

Each generalized displacement of the sector plate is represented by the modified Fourier series consisting of a standard Fourier cosine series and several auxiliary closed-form functions introduced to remove any potential discontinuity of the original displacement and its derivatives and accelerate the convergence of the series representation. The general boundary conditions of the sector plate are realized by using the artificial spring boundary technique which contains three groups of liner springs and two groups of rotation springs. The convergence, accuracy, and reliability of the presented solutions are validated by numerical examples and comparison of the present results with those available in the literature and obtained by using FEA method and numerous new results for the moderately thick FG sandwich sector plate with various boundary conditions, material and geometric parameters, and elastic foundations are presented. The effects of elastic boundary restraint parameters, power-law exponents, sector angles, material types, thickness schemes, and foundation coefficients on the frequency values are examined and discussed in detail. The main innovation point and conclusions can be drawn:

(1) Compared with other methods, the present method can easily obtain the vibration information of the

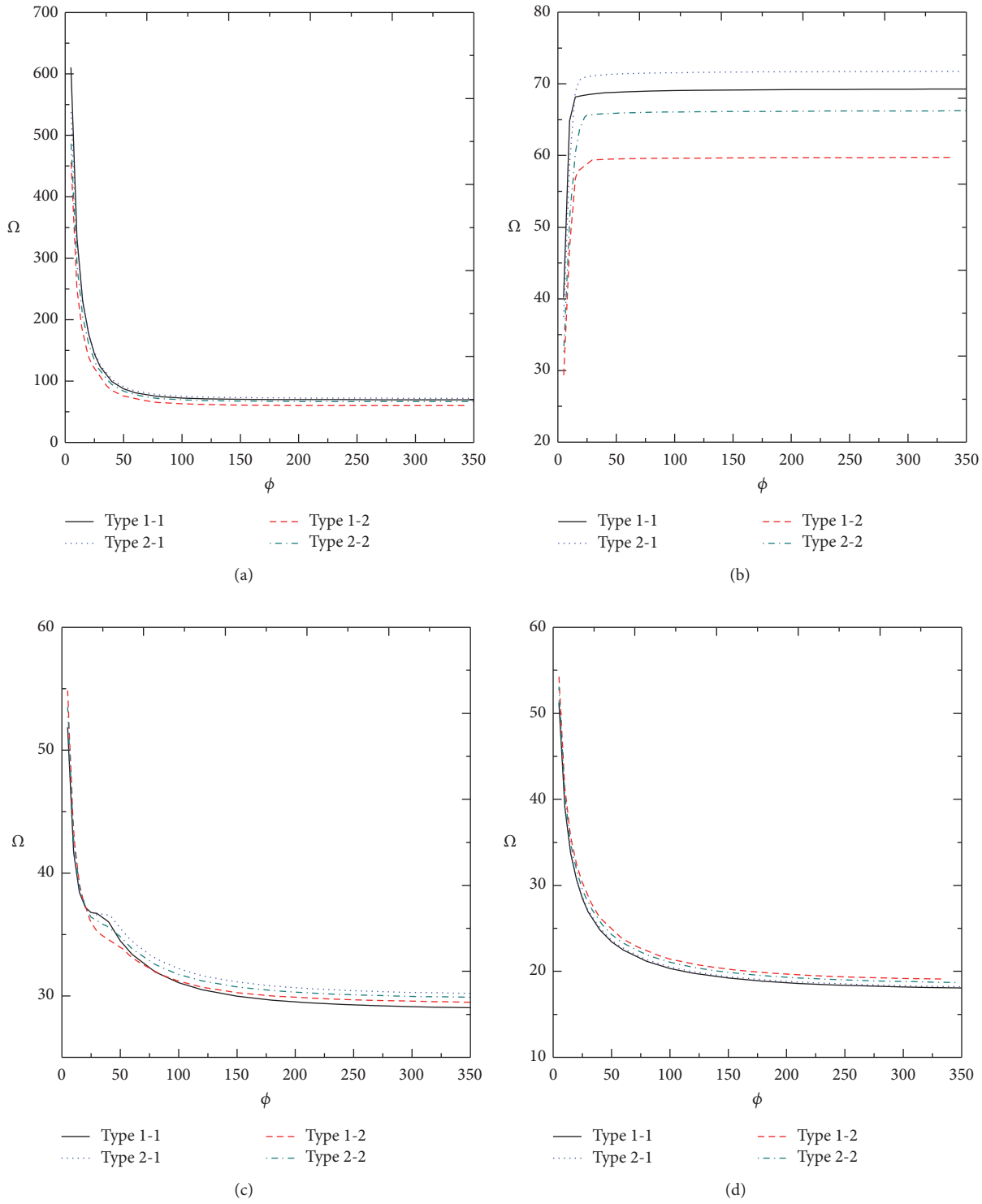

FIGURE 11: Variations of fundamental frequency parameter Ω of annular sector plate against different sector angles ($R_0/R_1 = 0.5$, $\phi = 120^\circ$, $h/R_1 = 0.2$, and $p^1 = p^3 = 5$): (a) CCCC; (b) CFCF; (c) $CE^1E^1E^1$; (d) $E^3E^3E^3E^3$.

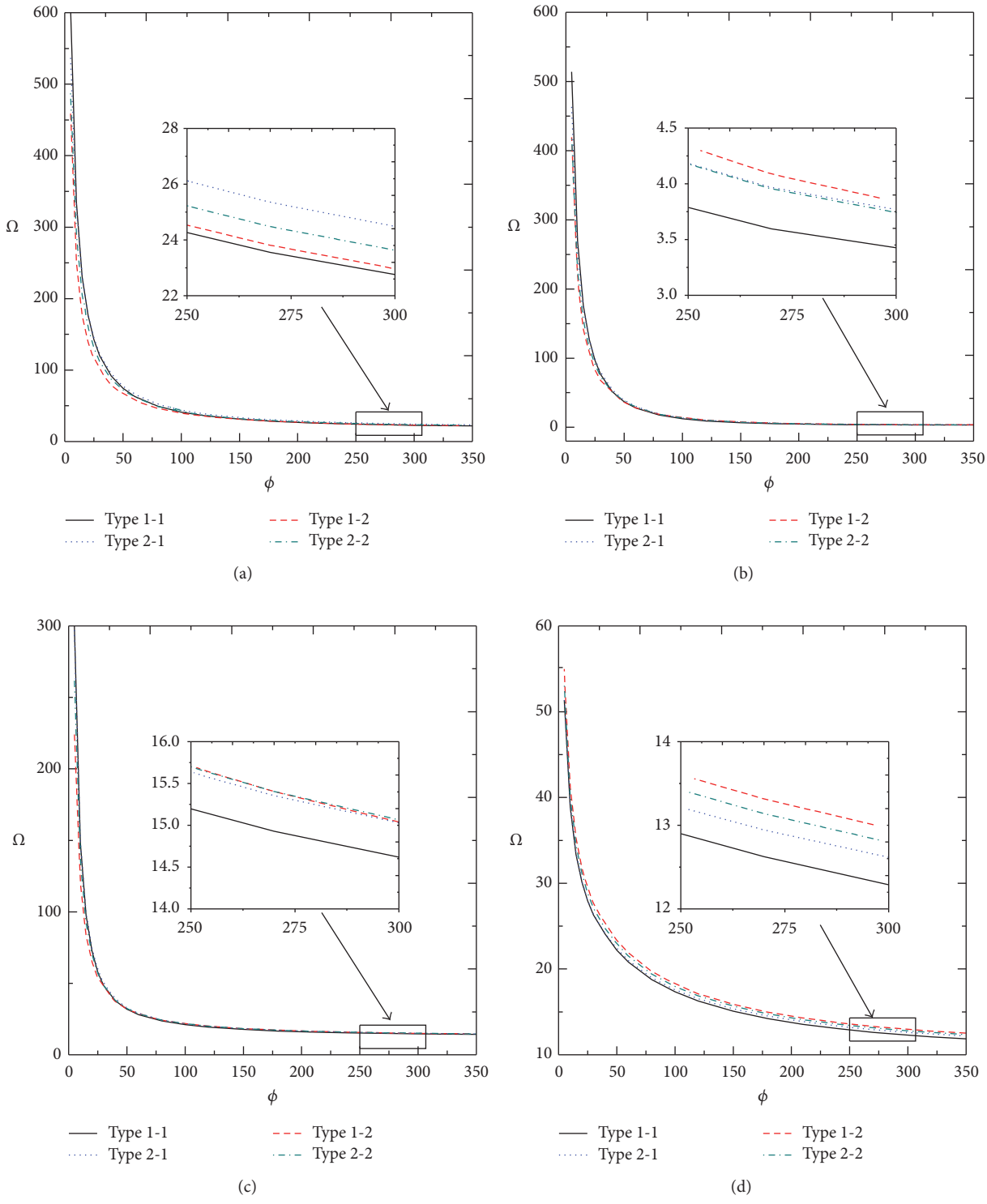

FIGURE 12: Variations of fundamental frequency parameter Ω of circular sector plate against different sector angles ($h/R_1 = 0.2$, $\phi = 120^\circ$, and $p^1 = p^3 = 5$, 2-2-1): (a) CCC (b) CFC; (c) CE^1E^1; (d) $E^3E^3E^3$.

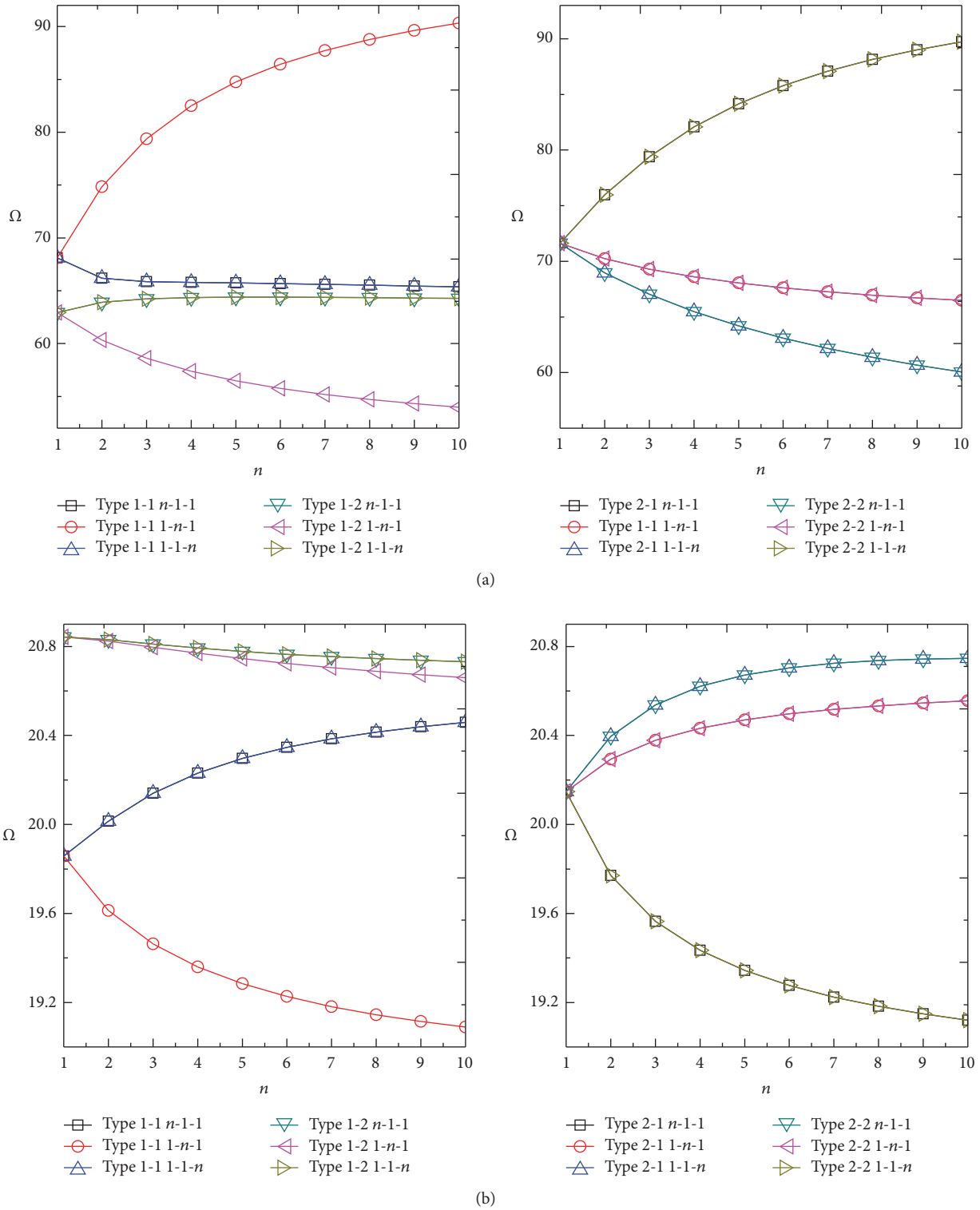

FIGURE 13: Variations of fundamental frequency parameter Ω of annular sector plate with material types and different thickness schemes ($R_0/R_1 = 0.5$, $\phi = 120^\circ$, $h/R_1 = 0.2$, and $p^1 = p^3 = 5$): (a) CCCC; (b) $E^3E^3E^3E^3$.

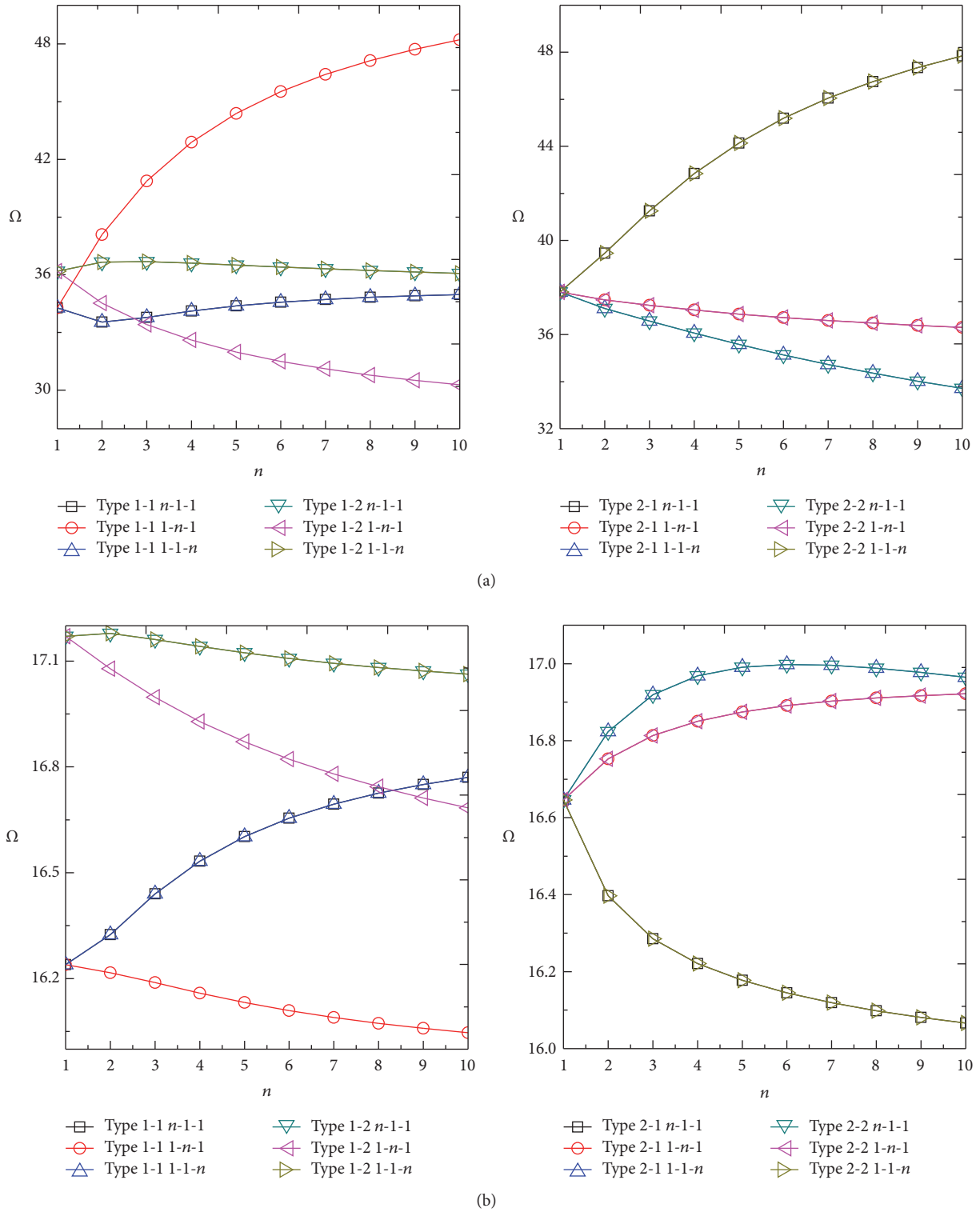

FIGURE 14: Variations of fundamental frequency parameter Ω of circular sector plate with material types and different thickness schemes ($\phi = 120^\circ$, $h/R_1 = 0.2$, and $p^1 = p^3 = 5$): (a) CCC; (b) $E^3E^3E^3$.

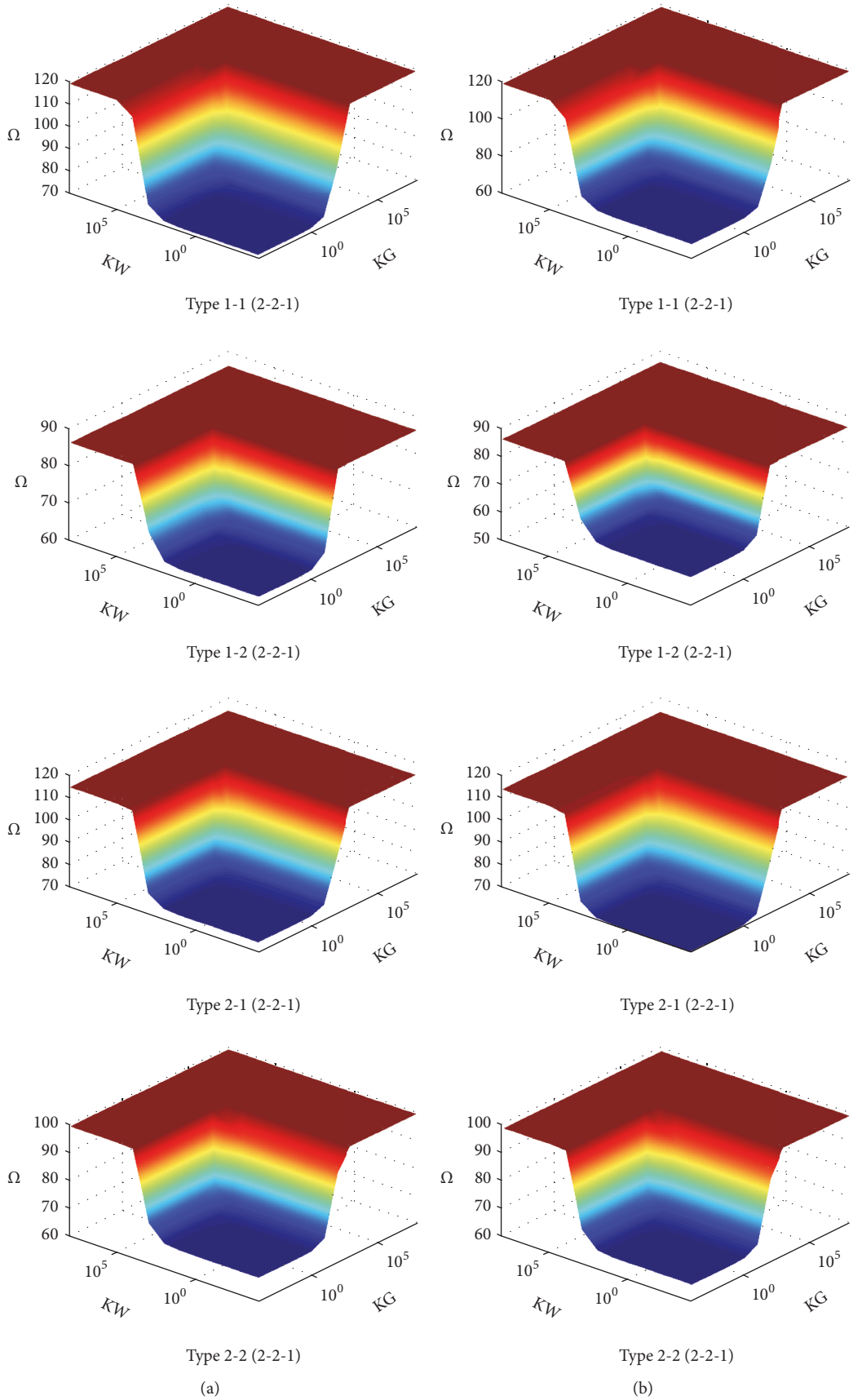

FIGURE 15: Variation of the frequency parameters Ω versus the elastic foundation coefficients for annular sector plates with different boundary conditions: (a) CCCC; (b) $E^2E^2E^2E^2$.

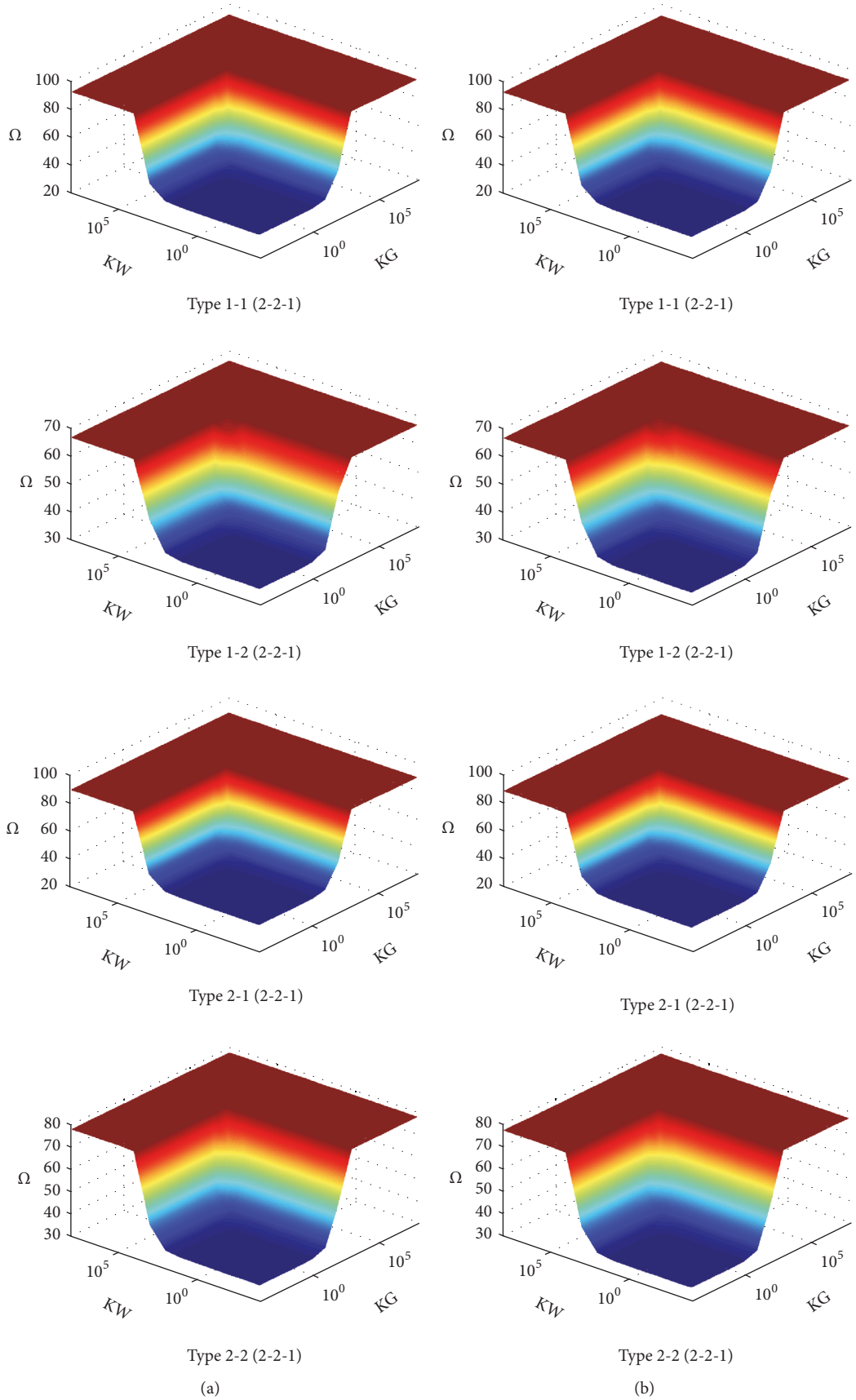

FIGURE 16: Variation of the frequency parameters Ω versus the elastic foundation coefficients for circular sector plates with different boundary conditions: (a) CCC; (b) $E^2E^2E^2$.

moderately thick FG sandwich sector plate with general boundary conditions and enables rapid convergence, high reliability, and accuracy.

(2) New results for moderately thick FG sandwich sector plates with various boundary conditions, material and geometric parameters, and elastic foundations are presented.

(3) The vibration characteristics of the moderately thick FG sandwich sector plate strongly depend on boundary conditions, power-law exponents, sector angles, material types, thickness schemes, and foundation coefficients.

Appendix

The submatrices of global stiffness and mass matrices of the plate are written by

$$\mathbf{K}_{uu} = \iint \left\{ A_{11} \frac{\partial \mathbf{U}^T}{\partial r} \frac{\partial \mathbf{U}}{\partial r} + A_{11} \frac{1}{r^2} \mathbf{U}^T \mathbf{U} + A_{66} \frac{1}{r^2} \cdot \frac{\partial \mathbf{U}^T}{\partial \theta} \frac{\partial \mathbf{U}}{\partial \theta} + A_{12} \frac{1}{r} \left(\frac{\partial \mathbf{U}^T}{\partial r} \mathbf{U} + \mathbf{U}^T \frac{\partial \mathbf{U}}{\partial r} \right) \right\} dS + \iint \left\{ R_0 k^u_{r\_0} \mathbf{U}^T \mathbf{U} \right\}_{|r=R_0} dS_0 + \iint \left\{ R_1 k^u_{r\_1} \mathbf{U}^T \mathbf{U} \right\}_{|r=R_1} dS_1 + \iint \left\{ k^u_{\deg\_0} \mathbf{U}^T \mathbf{U} \right\}_{|\theta=0} dS_2 + \iint \left\{ k^u_{\deg\_1} \mathbf{U}^T \mathbf{U} \right\}_{|\theta=\phi} dS_3$$

$$\mathbf{K}_{uv} = \iint \left\{ A_{11} \frac{1}{r^2} \left(\frac{\partial \mathbf{V}^T}{\partial \theta} \mathbf{U} + \frac{\partial \mathbf{V}}{\partial \theta} \mathbf{U}^T \right) + A_{66} \left(\frac{\partial \mathbf{V}^T}{\partial r} - \frac{\mathbf{V}^T}{r} \right) \frac{\partial \mathbf{U}}{r \partial \theta} + A_{66} \left(\frac{\partial \mathbf{V}}{\partial r} - \frac{\mathbf{V}}{r} \right) \frac{\partial \mathbf{U}^T}{r \partial \theta} + A_{12} \left(\frac{\partial \mathbf{U}^T}{\partial r} \frac{\partial \mathbf{V}}{r \partial \theta} + \frac{\partial \mathbf{U}}{\partial r} \frac{\partial \mathbf{V}^T}{r \partial \theta} \right) \right\} dS$$

$$\mathbf{K}_{u\psi_r} = \iint \left\{ B_{11} \frac{1}{r^2} \left(\mathbf{U}^T \mathbf{\Phi} + \mathbf{U} \mathbf{\Phi}^T \right) + B_{12} \frac{1}{r} \left(\mathbf{U}^T \frac{\partial \mathbf{\Phi}}{\partial r} + \mathbf{U} \frac{\partial \mathbf{\Phi}^T}{\partial r} \right) + B_{11} \left(\frac{\partial \mathbf{U}^T}{\partial r} \frac{\partial \mathbf{\Phi}}{\partial r} + \frac{\partial \mathbf{U}}{\partial r} \frac{\partial \mathbf{\Phi}^T}{\partial r} \right) + B_{12} \cdot \frac{1}{r} \left(\frac{\partial \mathbf{U}^T}{\partial r} \mathbf{\Phi} + \mathbf{\Phi}^T \frac{\partial \mathbf{U}}{\partial r} \right) + B_{66} \frac{1}{r^2} \left(\frac{\partial \mathbf{U}^T}{\partial \theta} \frac{\partial \mathbf{\Phi}}{\partial \theta} + \frac{\partial \mathbf{U}}{\partial \theta} \frac{\partial \mathbf{\Phi}^T}{\partial \theta} \right) \right\} dS$$

$$\mathbf{K}_{u\psi_\theta} = \iint \left\{ B_{11} \frac{1}{r^2} \left(\mathbf{U}^T \frac{\partial \mathbf{\Theta}}{\partial \theta} + \frac{\partial \mathbf{\Theta}^T}{\partial \theta} \mathbf{U} \right) + B_{12} \cdot \frac{1}{r} \left(\frac{\partial \mathbf{U}^T}{\partial r} \frac{\partial \mathbf{\Theta}}{\partial \theta} + \frac{\partial \mathbf{\Theta}^T}{\partial \theta} \frac{\partial \mathbf{U}}{\partial r} \right) + B_{66} \left[\frac{\partial \mathbf{U}^T}{r \partial \theta} \left(\frac{\partial \mathbf{\Theta}}{\partial r} - \frac{\mathbf{\Theta}}{r} \right) + \left(\frac{\partial \mathbf{\Theta}^T}{\partial r} - \frac{\mathbf{\Theta}^T}{r} \right) \frac{\partial \mathbf{U}}{r \partial \theta} \right] \right\} dS$$

$$\mathbf{K}_{vv} = \iint \left\{ A_{11} \frac{1}{r^2} \frac{\partial \mathbf{V}^T}{\partial \theta} \frac{\partial \mathbf{V}}{\partial \theta} + A_{66} \left(\frac{\partial \mathbf{V}^T}{\partial r} - \frac{\mathbf{V}^T}{r} \right) \cdot \left(\frac{\partial \mathbf{V}}{\partial r} - \frac{\mathbf{V}}{r} \right) \right\} dS + \iint \left\{ R_0 k^v_{r\_0} \mathbf{V}^T \mathbf{V} \right\}_{|r=R_0} dS_0 + \iint \left\{ R_1 k^v_{r\_1} \mathbf{V}^T \mathbf{V} \right\}_{|r=R_1} dS_1 + \iint \left\{ k^v_{\deg\_0} \mathbf{V}^T \mathbf{V} \right\}_{|\theta=0} dS_2 + \iint \left\{ k^v_{\deg\_1} \mathbf{V}^T \mathbf{V} \right\}_{|\theta=\phi} dS_3$$

$$\mathbf{K}_{v\psi_r} = \iint \left\{ B_{11} \frac{1}{r^2} \left(\frac{\partial \mathbf{V}^T}{\partial \theta} \mathbf{\Phi} + \mathbf{\Phi}^T \frac{\partial \mathbf{V}}{\partial \theta} \right) + B_{12} \cdot \frac{1}{r} \left(\frac{\partial \mathbf{V}^T}{\partial \theta} \frac{\partial \mathbf{\Phi}}{\partial r} + \frac{\partial \mathbf{\Phi}^T}{\partial r} \frac{\partial \mathbf{V}}{\partial \theta} \right) + B_{66} \left(\frac{\partial \mathbf{V}^T}{\partial r} \frac{\partial \mathbf{\Phi}}{r \partial \theta} + \frac{\partial \mathbf{\Phi}^T}{r \partial \theta} \frac{\partial \mathbf{V}}{\partial r} \right) - B_{66} \left(\frac{\mathbf{V}^T}{r} \frac{\partial \mathbf{\Phi}}{r \partial \theta} + \frac{\partial \mathbf{\Phi}^T}{r \partial \theta} \frac{\mathbf{V}}{r} \right) \right\} dS$$

$$\mathbf{K}_{v\psi_\theta} = \iint \left\{ B_{11} \frac{1}{r^2} \left(\frac{\partial \mathbf{V}^T}{\partial \theta} \frac{\partial \mathbf{\Theta}}{\partial \theta} + \frac{\partial \mathbf{V}}{\partial \theta} \frac{\partial \mathbf{\Theta}^T}{\partial \theta} \right) + B_{66} \left(\frac{\partial \mathbf{V}^T}{\partial r} - \frac{\mathbf{V}^T}{r} \right) \left(\frac{\partial \mathbf{\Theta}}{\partial r} - \frac{\mathbf{\Theta}}{r} \right) + B_{66} \left(\frac{\partial \mathbf{\Theta}^T}{\partial r} - \frac{\mathbf{\Theta}^T}{r} \right) \left(\frac{\partial \mathbf{V}}{\partial r} - \frac{\mathbf{V}}{r} \right) \right\} dS$$

$$\mathbf{K}_{ww} = \iint \left\{ \kappa A_{66} \frac{\partial \mathbf{W}^T}{\partial r} \frac{\partial \mathbf{W}}{\partial r} + \kappa A_{66} \frac{1}{r^2} \frac{\partial \mathbf{W}^T}{\partial \theta} \cdot \frac{\partial \mathbf{W}}{\partial \theta} \right\} dS + \iint \left\{ R_0 k^w_{r\_0} \mathbf{W}^T \mathbf{W} \right\}_{|r=R_0} dS_0 + \iint \left\{ R_1 k^w_{r\_1} \mathbf{W}^T \mathbf{W} \right\}_{|r=R_1} dS_1 + \iint \left\{ k^w_{\deg\_0} \mathbf{W}^T \mathbf{W} \right\}_{|\theta=0} dS_2$$

$$+\iint\left\{k^{w}_{\deg\_1}\mathbf{W}^{T}\mathbf{W}\right\}_{|\theta=\phi}dS_3+\iint\left\{K_w\mathbf{W}^{T}\mathbf{W}+K_s\frac{\partial\mathbf{W}^{T}}{\partial r}\frac{\partial\mathbf{W}}{\partial r}+K_s\frac{1}{r^2}\frac{\partial\mathbf{W}^{T}}{\partial\theta}\frac{\partial\mathbf{W}}{\partial\theta}\right\}dS$$

$$\mathbf{K}_{w\psi_r}=\iint\left\{\kappa A_{66}\left(\frac{\partial\mathbf{W}^{T}}{\partial r}\mathbf{\Phi}+\mathbf{\Phi}^{T}\frac{\partial\mathbf{W}}{\partial r}\right)\right\}dS,$$

$$\mathbf{K}_{w\psi_\theta}=\iint\left\{\kappa A_{66}\frac{1}{r}\left(\frac{\partial\mathbf{W}^{T}}{\partial\theta}\mathbf{\Theta}+\mathbf{\Theta}^{T}\frac{\partial\mathbf{W}}{\partial\theta}\right)\right\}dS$$

$$\mathbf{K}_{\psi_r\psi_r}=\iint\left\{\kappa A_{66}\mathbf{\Phi}^{T}\mathbf{\Phi}+D_{12}\frac{1}{r}\left(\frac{\partial\mathbf{\Phi}^{T}}{\partial r}\mathbf{\Phi}+\mathbf{\Phi}^{T}\frac{\partial\mathbf{\Phi}}{\partial r}\right)+D_{11}\left(\frac{\partial\mathbf{\Phi}^{T}}{\partial r}\frac{\partial\mathbf{\Phi}}{\partial r}+\frac{1}{r^2}\mathbf{\Phi}^{T}\mathbf{\Phi}\right)+D_{66}\cdot\frac{1}{r^2}\frac{\partial\mathbf{\Phi}^{T}}{\partial\theta}\frac{\partial\mathbf{\Phi}}{\partial\theta}\right\}dS+\iint\left\{R_0K^{r}_{r\_0}\mathbf{\Phi}^{T}\mathbf{\Phi}\right\}_{|r=R_0}dS_0+\iint\left\{R_1K^{r}_{r\_1}\mathbf{\Phi}^{T}\mathbf{\Phi}\right\}_{|r=R_1}dS_1+\iint\left\{K^{r}_{\deg\_0}\mathbf{\Phi}^{T}\mathbf{\Phi}\right\}_{|\theta=0}dS_2+\iint\left\{K^{r}_{\deg\_1}\mathbf{\Phi}^{T}\mathbf{\Phi}\right\}_{|\theta=\phi}dS_3$$

$$\mathbf{K}_{\psi_r\psi_\theta}=\iint\left\{D_{12}\frac{1}{r}\left(\frac{\partial\mathbf{\Phi}^{T}}{\partial r}\frac{\partial\mathbf{\Theta}}{\partial\theta}+\frac{\partial\mathbf{\Phi}}{\partial r}\frac{\partial\mathbf{\Theta}^{T}}{\partial\theta}\right)+D_{11}\cdot\frac{1}{r}\left(\frac{\partial\mathbf{\Theta}^{T}}{\partial\theta}\frac{\mathbf{\Phi}}{r}+\frac{\partial\mathbf{\Theta}}{\partial\theta}\frac{\mathbf{\Phi}^{T}}{r}\right)+D_{66}\cdot\frac{1}{r}\left(\frac{\partial\mathbf{\Phi}^{T}}{\partial\theta}\left(\frac{\partial\mathbf{\Theta}}{\partial r}-\frac{\mathbf{\Theta}}{r}\right)+\frac{\partial\mathbf{\Phi}}{\partial\theta}\left(\frac{\partial\mathbf{\Theta}^{T}}{\partial r}-\frac{\mathbf{\Theta}^{T}}{r}\right)\right)\right\}dS$$

$$\mathbf{K}_{\psi_\theta\psi_\theta}=\iint\left\{\kappa A_{66}\mathbf{\Theta}^{T}\mathbf{\Theta}+D_{11}\frac{1}{r^2}\frac{\partial\mathbf{\Theta}^{T}}{\partial\theta}\frac{\partial\mathbf{\Theta}}{\partial\theta}+D_{66}\left(\frac{\partial\mathbf{\Theta}^{T}}{\partial r}-\frac{\mathbf{\Theta}^{T}}{r}\right)\left(\frac{\partial\mathbf{\Theta}}{\partial r}-\frac{\mathbf{\Theta}}{r}\right)\right\}dS+\iint\left\{R_0K^{\theta}_{r\_0}\mathbf{\Theta}^{T}\mathbf{\Theta}\right\}_{|r=R_0}dS_0+\iint\left\{R_1K^{\theta}_{r\_1}\mathbf{\Theta}^{T}\mathbf{\Theta}\right\}_{|r=R_1}dS_1+\iint\left\{K^{\theta}_{\deg\_0}\mathbf{\Theta}^{T}\mathbf{\Theta}\right\}_{|\theta=0}dS_2+\iint\left\{K^{\theta}_{\deg\_1}\mathbf{\Theta}^{T}\mathbf{\Theta}\right\}_{|\theta=\phi}dS_3$$

$$\mathbf{M}_{uu}=\iint\left\{I_0\mathbf{U}^{T}\mathbf{U}\right\}dS;$$

$$\mathbf{M}_{vv}=\iint\left\{I_0\mathbf{V}^{T}\mathbf{V}\right\}dS;$$

$$\mathbf{M}_{ww}=\iint\left\{I_0\mathbf{W}^{T}\mathbf{W}\right\}dS$$

$$\mathbf{M}_{\varphi\varphi}=\iint\left\{I_2\mathbf{\Phi}^{T}\mathbf{\Phi}\right\}dS;$$

$$\mathbf{M}_{\theta\theta}=\iint\left\{I_2\mathbf{\Theta}^{T}\mathbf{\Theta}\right\}dS;$$

$$\mathbf{M}_{u\varphi}=\iint\left\{I_0\left(\mathbf{U}^{T}\mathbf{\Phi}+\mathbf{U}\mathbf{\Phi}^{T}\right)\right\}dS;$$

$$\mathbf{M}_{v\theta}=\iint\left\{I_0\left(\mathbf{V}^{T}\mathbf{\Theta}+\mathbf{V}\mathbf{\Phi}^{T}\right)\right\}dS,\tag{A.1}$$

where

$$\mathbf{U}=\left\{\begin{array}{c}\cos\lambda_{R0}r,\ldots,\cos\lambda_{R0}r\cos\lambda_{\phi n}\theta,\ldots,\cos\lambda_{RM}r\cos\lambda_{\phi N}\theta,\\ \zeta^1_b(\theta),\ldots,\zeta^1_b(\theta)\cos\lambda_{Rm}r,\ldots,\zeta^2_b(\theta)\cos\lambda_{RM}r,\\ \zeta^1_a(r),\ldots,\zeta^1_a(r)\cos\lambda_{\phi n}\theta,\ldots,\zeta^2_a(r)\cos\lambda_{\phi N}\theta,\end{array}\right\}\tag{A.2}$$

$\mathbf{V}=\mathbf{W}=\mathbf{\Phi}=\mathbf{\Theta}=\mathbf{U}$.

Conflicts of Interest

The authors declare that they have no conflicts of interest.

Funding

This study was funded by the National Key Research and Development Program of China (2016YFC0303406), Assembly Advanced Research Fund of China (6140210020105), Major Innovation Projects of High Technology Ship Funds of Ministry of Industry and Information of China, National Natural Science Foundation of China (no. 51209052), High Technology Ship Funds of Ministry of Industry and Information Technology of China, Fundamental Research Funds for the Central Universities (HEUCFD1515, HEUCFM170113), and China Postdoctoral Science Foundation (2014M552661).

References

[1] H. Zafarmand and M. Kadkhodayan, "Three dimensional elasticity solution for static and dynamic analysis of multi-directional functionally graded thick sector plates with general boundary conditions," *Composites Part B: Engineering*, vol. 69, pp. 592–602, 2015.

[2] R. Q. Xu, "Three-dimensional exact solutions for the free vibration of laminated transversely isotropic circular, annular and sectorial plates with unusual boundary conditions," *Archive of Applied Mechanics*, vol. 78, no. 7, pp. 543–558, 2008.

[3] V. Tahouneh and M. H. Yas, "3-D free vibration analysis of thick functionally graded annular sector plates on Pasternak

elastic foundation via 2-D Differential quadrature method," *Acta Mechanica*, vol. 223, no. 9, pp. 1879–1897, 2012.

[4] M. Tahani and S. M. Mousavi, "Analytical solution for bending problem of moderately thick composite annular sector plates with general boundary conditions and loadings using multi-term extended Kantorovich method," *Archive of Applied Mechanics*, vol. 83, no. 6, pp. 969–985, 2013.

[5] Z. Su, G. Jin, and X. Wang, "Free vibration analysis of laminated composite and functionally graded sector plates with general boundary conditions," *Composite Structures*, vol. 132, pp. 720–736, 2015.

[6] R. S. Srinivasan and V. Thiruvenkatachari, "Free vibration analysis of laminated annular sector plates," *Journal of Sound and Vibration*, vol. 109, no. 1, pp. 89–96, 1986.

[7] A. Sharma, H. B. Sharda, and Y. Nath, "Stability and vibration of thick laminated composite sector plates," *Journal of Sound and Vibration*, vol. 287, no. 1-2, pp. 1–23, 2005.

[8] A. Sharma, "Free vibration of moderately thick antisymmetric laminated annular sector plates with elastic edge constraints," *International Journal of Mechanical Sciences*, vol. 83, pp. 124–132, 2014.

[9] A. R. Saidi, F. Hejripour, and E. Jomehzadeh, "On the stress singularities and boundary layer in moderately thick functionally graded sectorial plates," *Applied Mathematical Modelling*, vol. 34, no. 11, pp. 3478–3492, 2010.

[10] A. R. Saidi, E. Jomehzadeh, and S. R. Atashipour, "Exact analytical solution for bending analysis of functionally graded annular sector plates," *International Journal of Engineering, Transactions A: Basics*, vol. 22, no. 3, pp. 307–316, 2009.

[11] A. R. Saidi and A. Hasani Baferani, "Thermal buckling analysis of moderately thick functionally graded annular sector plates," *Composite Structures*, vol. 92, no. 7, pp. 1744–1752, 2010.

[12] S. Sahraee, "Bending analysis of functionally graded sectorial plates using Levinson plate theory," *Composite Structures*, vol. 88, no. 4, pp. 548–557, 2009.

[13] S. Panda and G. G. Sopan, "Nonlinear analysis of smart functionally graded annular sector plates using cylindrically orthotropic piezoelectric fiber reinforced composite," *International Journal of Mechanics and Materials in Design*, vol. 9, no. 1, pp. 35–53, 2013.

[14] H. R. Noori, E. Jomehzadeh, and A. R. Saidi, "On the stretching and bending analyses of thin functionally graded annular sector plates," in *Materials with Complex Behaviour II*, vol. 16 of *Advanced Structured Materials*, pp. 433–446, Springer, Berlin, Germany, 2012.

[15] A. Naderi and A. R. Saidi, "Exact solution for stability analysis of moderately thick functionally graded sector plates on elastic foundation," *Composite Structures*, vol. 93, no. 2, pp. 629–638, 2011.

[16] A. Naderi and A. R. Saidi, "An analytical solution for buckling of moderately thick functionally graded sector and annular sector plates," *Archive of Applied Mechanics*, vol. 81, no. 6, pp. 809–828, 2011.

[17] A. Naderi and A. R. Saidi, "Buckling analysis of functionally graded annular sector plates resting on elastic foundations," *Proceedings of the Institution of Mechanical Engineers, Part C: Journal of Mechanical Engineering Science*, vol. 225, no. 2, pp. 312–325, 2011.

[18] S. M. Mousavi and M. Tahani, "Analytical solution for bending of moderately thick radially functionally graded sector plates with general boundary conditions using multi-term extended Kantorovich method," *Composites Part B: Engineering*, vol. 43, no. 3, pp. 1405–1416, 2012.

[19] M. Mehrabian and M. E. Golmakani, "Nonlinear bending analysis of radial-stiffened annular laminated sector plates with dynamic relaxation method," *Computers and Mathematics with Applications*, vol. 69, no. 10, pp. 1272–1302, 2015.

[20] P. Malekzadeh, "Three-dimensional free vibration analysis of thick laminated annular sector plates using a hybrid method," *Composite Structures*, vol. 90, no. 4, pp. 428–437, 2009.

[21] S. Maleki and M. Tahani, "Bending analysis of laminated sector plates with polar and rectilinear orthotropy," *European Journal of Mechanics. A. Solids*, vol. 40, pp. 84–96, 2013.

[22] X. Liang, H.-L. Kou, L. Wang, A. C. Palmer, Z. Wang, and G. Liu, "Three-dimensional transient analysis of functionally graded material annular sector plate under various boundary conditions," *Composite Structures*, vol. 132, pp. 584–596, 2015.

[23] E. Jomehzadeh, A. R. Saidi, and S. R. Atashipour, "An analytical approach for stress analysis of functionally graded annular sector plates," *Materials and Design*, vol. 30, no. 9, pp. 3679–3685, 2009.

[24] G. Jin, Z. Su, T. Ye, and S. Gao, "Three-dimensional free vibration analysis of functionally graded annular sector plates with general boundary conditions," *Composites Part B: Engineering*, vol. 83, pp. 352–366, 2014.

[25] A. Houmat, "Large amplitude free vibration of shear deformable laminated composite annular sector plates by a sector p-element," *International Journal of Non-Linear Mechanics*, vol. 43, no. 9, pp. 834–843, 2008.

[26] S. Hosseini-Hashemi, H. Akhavan, H. R. D. Taher, N. Daemi, and A. Alibeigloo, "Differential quadrature analysis of functionally graded circular and annular sector plates on elastic foundation," *Materials and Design*, vol. 31, no. 4, pp. 1871–1880, 2010.

[27] M. E. Golmakani and M. Kadkhodayan, "Large deflection thermoelastic analysis of functionally graded stiffened annular sector plates," *International Journal of Mechanical Sciences*, vol. 69, pp. 94–106, 2013.

[28] M. E. Golmakani and J. Alamatian, "Large deflection analysis of shear deformable radially functionally graded sector plates on two-parameter elastic foundations," *European Journal of Mechanics. A. Solids*, vol. 42, pp. 251–265, 2013.

[29] A. Fereidoon, A. Mohyeddin, M. Sheikhi, and H. Rahmani, "Bending analysis of functionally graded annular sector plates by extended Kantorovich method," *Composites Part B: Engineering*, vol. 43, no. 5, pp. 2172–2179, 2012.

[30] S. R. Falahatgar and M. Salehi, "Dynamic relaxation nonlinear viscoelastic analysis of annular sector composite plate," *Journal of Composite Materials*, vol. 43, no. 3, pp. 257–275, 2009.

[31] Y. K. Cheung and W. L. Kwok, "Dynamic analysis of circular and sector thick, layered plates," *Journal of Sound and Vibration*, vol. 42, no. 2, pp. 147–158, 1975.

[32] S. A. Belalia and A. Houmat, "Nonlinear free vibration of functionally graded shear deformable sector plates by a curved triangular p-element," *European Journal of Mechanics. A. Solids*, vol. 35, pp. 1–9, 2012.

[33] A. H. Baferani, A. R. Saidi, and E. Jomehzadeh, "Exact analytical solution for free vibration of functionally graded thin annular sector plates resting on elastic foundation," *Journal of Vibration and Control*, vol. 18, no. 2, pp. 246–267, 2012.

[34] K. Asemi, M. Salehi, and M. Akhlaghi, "Three dimensional biaxial buckling analysis of functionally graded annular sector

plate fully or partially supported on Winkler elastic foundation," *Aerospace Science and Technology*, vol. 39, pp. 426–441, 2014.

[35] A. Andakhshideh, S. Maleki, and M. M. Aghdam, "Non-linear bending analysis of laminated sector plates using generalized differential quadrature," *Composite Structures*, vol. 92, no. 9, pp. 2258–2264, 2010.

[36] F. Alinaghizadeh and M. Kadkhodayan, "Investigation of non-linear bending analysis of moderately thick functionally graded material sector plates subjected to thermomechanical loads by the GDQ method," *Journal of Engineering Mechanics*, vol. 140, no. 5, article 04014012, 2014.

[37] M. M. Aghdam, N. Shahmansouri, and M. Mohammadi, "Extended Kantorovich method for static analysis of moderately thick functionally graded sector plates," *Mathematics and Computers in Simulation*, vol. 86, pp. 118–130, 2012.

[38] A. R. Saidi, A. H. Baferani, and E. Jomehzadeh, "Benchmark solution for free vibration of functionally graded moderately thick annular sector plates," *Acta Mechanica*, vol. 219, no. 3-4, pp. 309–335, 2011.

[39] S. Mirtalaie, M. Hajabasi, and F. Hejripour, "Free vibration analysis of functionally graded moderately thick annular sector plates using differential quadrature method," in *Applied Mechanics and Materials*, Trans Tech Publications, 2012.

[40] A. M. Zenkour, "A comprehensive analysis of functionally graded sandwich plates: part 2. Buckling and free vibration," *International Journal of Solids and Structures*, vol. 42, no. 18-19, pp. 5243–5258, 2005.

[41] K. M. Liew, J. Yang, and Y. F. Wu, "Nonlinear vibration of a coating-FGM-substrate cylindrical panel subjected to a temperature gradient," *Computer Methods in Applied Mechanics and Engineering*, vol. 195, no. 9-12, pp. 1007–1026, 2006.

[42] S. Kapuria, M. Bhattacharyya, and A. N. Kumar, "Bending and free vibration response of layered functionally graded beams: a theoretical model and its experimental validation," *Composite Structures*, vol. 82, no. 3, pp. 390–402, 2008.

[43] Q. Li, V. P. Iu, and K. P. Kou, "Three-dimensional vibration analysis of functionally graded material sandwich plates," *Journal of Sound and Vibration*, vol. 311, no. 1-2, pp. 498–515, 2008.

[44] H. J. Xiang and J. Yang, "Free and forced vibration of a laminated FGM Timoshenko beam of variable thickness under heat conduction," *Composites—Part B: Engineering*, vol. 39, no. 2, pp. 292–303, 2008.

[45] M. Kashtalyan and M. Menshykova, "Three-dimensional elasticity solution for sandwich panels with a functionally graded core," *Composite Structures*, vol. 87, no. 1, pp. 36–43, 2009.

[46] S. C. Pradhan and T. Murmu, "Thermo-mechanical vibration of FGM sandwich beam under variable elastic foundations using differential quadrature method," *Journal of Sound and Vibration*, vol. 321, no. 1-2, pp. 342–362, 2009.

[47] M. Cinefra, S. Belouettar, M. Soave, and E. Carrera, "Variable kinematic models applied to free-vibration analysis of functionally graded material shells," *European Journal of Mechanics, A/Solids*, vol. 29, no. 6, pp. 1078–1087, 2010.

[48] N. El Meiche, A. Tounsi, N. Ziane, I. Mechab, and E. A. Adda.Bedia, "A new hyperbolic shear deformation theory for buckling and vibration of functionally graded sandwich plate," *International Journal of Mechanical Sciences*, vol. 53, no. 4, pp. 237–247, 2011.

[49] L. Hadji, H. A. Atmane, A. Tounsi, I. Mechab, and E. A. Adda Bedia, "Free vibration of functionally graded sandwich plates using four-variable refined plate theory," *Applied Mathematics and Mechanics. English Edition*, vol. 32, no. 7, pp. 925–942, 2011.

[50] S. Natarajan and G. Manickam, "Bending and vibration of functionally graded material sandwich plates using an accurate theory," *Finite Elements in Analysis and Design*, vol. 57, pp. 32–42, 2012.

[51] A. M. A. Neves, A. J. M. Ferreira, E. Carrera et al., "Static, free vibration and buckling analysis of isotropic and sandwich functionally graded plates using a quasi-3D higher-order shear deformation theory and a meshless technique," *Composites Part B: Engineering*, vol. 44, no. 1, pp. 657–674, 2013.

[52] M. Sobhy, "Buckling and free vibration of exponentially graded sandwich plates resting on elastic foundations under various boundary conditions," *Composite Structures*, vol. 99, pp. 76–87, 2013.

[53] A. Alibeigloo and K. M. Liew, "Free vibration analysis of sandwich cylindrical panel with functionally graded core using three-dimensional theory of elasticity," *Composite Structures*, vol. 113, no. 1, pp. 23–30, 2014.

[54] F. A. Fazzolari and E. Carrera, "Refined hierarchical kinematics quasi-3D Ritz models for free vibration analysis of doubly curved FGM shells and sandwich shells with FGM core," *Journal of Sound and Vibration*, vol. 333, no. 5, pp. 1485–1508, 2014.

[55] P. Malekzadeh and M. Ghaedsharaf, "Three-dimensional free vibration of laminated cylindrical panels with functionally graded layers," *Composite Structures*, vol. 108, no. 1, pp. 894–904, 2014.

[56] H.-T. Thai, T.-K. Nguyen, T. P. Vo, and J. Lee, "Analysis of functionally graded sandwich plates using a new first-order shear deformation theory," *European Journal of Mechanics. A. Solids*, vol. 45, pp. 211–225, 2014.

[57] G. Jin, S. Shi, Z. Su, S. Li, and Z. Liu, "A modified Fourier–Ritz approach for free vibration analysis of laminated functionally graded shallow shells with general boundary conditions," *International Journal of Mechanical Sciences*, vol. 93, pp. 256–269, 2015.

[58] W. L. Li, "Free vibrations of beams with general boundary conditions," *Journal of Sound and Vibration*, vol. 237, no. 4, pp. 709–725, 2000.

[59] W. L. Li, "Comparison of fourier sine and cosine series expansions for beams with arbitrary boundary conditions," *Journal of Sound and Vibration*, vol. 255, no. 1, pp. 185–194, 2003.

[60] D. Shi, Q. Wang, X. Shi, and F. Pang, "An accurate solution method for the vibration analysis of Timoshenko beams with general elastic supports," *Proceedings of the Institution of Mechanical Engineers Part C: Journal of Mechanical Engineering Science*, pp. 2327–2340, 2014.

[61] D. Shao, S. Hu, Q. Wang, and F. Pang, "Free vibration of refined higher-order shear deformation composite laminated beams with general boundary conditions," *Composites Part B: Engineering*, vol. 108, pp. 75–90, 2017.

[62] W. L. Li, "A new method for structural model updating and joint stiffness identification," *Mechanical Systems and Signal Processing*, vol. 16, no. 1, pp. 155–167, 2002.

[63] Q. Wang, D. Shi, and Q. Liang, "Free vibration analysis of axially loaded laminated composite beams with general boundary conditions by using a modified Fourier-Ritz approach," *Journal of Composite Materials*, vol. 50, no. 15, pp. 2111–2135, 2016.

[64] D. Shi, Q. Wang, X. Shi, and F. Pang, "A series solution for the in-plane vibration analysis of orthotropic rectangular plates with non-uniform elastic boundary constraints and internal line supports," *Archive of Applied Mechanics*, vol. 85, no. 1, pp. 51–73, 2015.

[65] D. Shao, F. Hu, Q. Wang, F. Pang, and S. Hu, "Transient response analysis of cross-ply composite laminated rectangular plates with general boundary restraints by the method of reverberation ray matrix," *Composite Structures*, vol. 152, pp. 168–182, 2016.

[66] D. Shi, Q. Liang, Q. Wang, and X. Teng, "A unified solution for free vibration of orthotropic circular, annular and sector plates with general boundary conditions," *Journal of Vibroengineering*, vol. 18, no. 5, pp. 3138–3152, 2016.

[67] D. Shi, X. Lv, Q. Wang, and Q. Liang, "A unified solution for free vibration of orthotropic annular sector thin plates with general boundary conditions, internal radial line and circumferential arc supports," *Journal of Vibroengineering*, vol. 18, no. 1, pp. 361–377, 2016.

[68] X. Shi, D. Shi, W. L. Li, and Q. Wang, "A unified method for free vibration analysis of circular, annular and sector plates with arbitrary boundary conditions," *Journal of Vibration and Control*, vol. 22, no. 2, pp. 442–456, 2016.

[69] Q. Wang, D. Shi, Q. Liang, and F. Ahad, "An improved Fourier series solution for the dynamic analysis of laminated composite annular, circular, and sector plate with general boundary conditions," *Journal of Composite Materials*, vol. 50, no. 30, pp. 4199–4233, 2016.

[70] Q. Wang, D. Shi, Q. Liang, and F. e Ahad, "A unified solution for free in-plane vibration of orthotropic circular, annular and sector plates with general boundary conditions," *Applied Mathematical Modelling*, vol. 40, no. 21-22, pp. 9228–9253, 2016.

[71] Q. Wang, D. Shi, Q. Liang, and X. Shi, "A unified solution for vibration analysis of functionally graded circular, annular and sector plates with general boundary conditions," *Composites Part B: Engineering*, vol. 88, pp. 264–294, 2016.

[72] Q. Wang, D. Shi, and X. Shi, "A modified solution for the free vibration analysis of moderately thick orthotropic rectangular plates with general boundary conditions, internal line supports and resting on elastic foundation," *Meccanica*, vol. 51, no. 8, pp. 1985–2017, 2016.

[73] Q. Wang, F. Pang, B. Qin, and Q. Liang, "A unified formulation for free vibration of functionally graded carbon nanotube reinforced composite spherical panels and shells of revolution with general elastic restraints by means of the Rayleigh-Ritz method," *Polymer Composites*, 2017.

[74] Q. Wang, D. Shi, Q. Liang, and F. Pang, "A unified solution for vibration analysis of moderately thick, functionally graded rectangular plates with general boundary restraints and internal line supports," *Mechanics of Advanced Materials and Structures*, vol. 24, no. 11, pp. 961–973, 2017.

[75] H. Zhang, D. Shi, and Q. Wang, "An improved Fourier series solution for free vibration analysis of the moderately thick laminated composite rectangular plate with non-uniform boundary conditions," *International Journal of Mechanical Sciences*, vol. 121, pp. 1–20, 2017.

[76] K. Zhang, D. Shi, W. Wang, and Q. Wang, "Mechanical characterization of hybrid lattice-to-steel joint with pyramidal CFRP truss for marine application," *Composite Structures*, vol. 160, pp. 1198–1204, 2017.

[77] D. Shi, Y. Zhao, Q. Wang, X. Teng, and F. Pang, "A unified spectro-geometric-ritz method for vibration analysis of open and closed shells with arbitrary boundary conditions," *Shock and Vibration*, vol. 2016, Article ID 4097123, 30 pages, 2016.

[78] D. Shao, S. Hu, Q. Wang, and F. Pang, "An enhanced reverberation-ray matrix approach for transient response analysis of composite laminated shallow shells with general boundary conditions," *Composite Structures*, vol. 162, pp. 133–155, 2017.

[79] Q. Wang, B. Qin, D. Shi, and Q. Liang, "A semi-analytical method for vibration analysis of functionally graded carbon nanotube reinforced composite doubly-curved panels and shells of revolution," *Composite Structures*, vol. 174, pp. 87–109, 2017.

[80] Q. Wang, D. Shi, Q. Liang, and F. Pang, "Free vibrations of composite laminated doubly-curved shells and panels of revolution with general elastic restraints," *Applied Mathematical Modelling*, vol. 46, pp. 227–262, 2017.

[81] Q. Wang, D. Shi, Q. Liang, and F. Pang, "Free vibration of four-parameter functionally graded moderately thick doubly-curved panels and shells of revolution with general boundary conditions," *Applied Mathematical Modelling*, vol. 42, pp. 705–734, 2017.

[82] Q. Wang, D. Shi, F. Pang, and F. e Ahad, "Benchmark solution for free vibration of thick open cylindrical shells on Pasternak foundation with general boundary conditions," *Meccanica*, vol. 52, no. 1-2, pp. 457–482, 2017.

[83] H. Zhang, D. Shi, Q. Wang, and B. Qin, "Free vibration of functionally graded parabolic and circular panels with general boundary conditions," *Curved and Layered Structures*, vol. 4, no. 1, pp. 52–84, 2017.

[84] H. Xu and W. L. Li, "Dynamic behavior of multi-span bridges under moving loads with focusing on the effect of the coupling conditions between spans," *Journal of Sound and Vibration*, vol. 312, no. 4-5, pp. 736–753, 2008.

[85] Y. H. Chen, G. Jin, J. Du, and Z. Liu, "Power transmission analysis of coupled rectangular plates with elastically restrained coupling edge including in-plane vibration," in *Proceedings of the 20th International Congress on Acoustics, ICA 2010*, pp. 1–7, Sydney, Australia, 2010.

[86] J. Du, W. L. Li, Z. Liu, T. Yang, and G. Jin, "Free vibration of two elastically coupled rectangular plates with uniform elastic boundary restraints," *Journal of Sound and Vibration*, vol. 330, no. 4, pp. 788–804, 2011.

[87] Y. Chen, G. Jin, M. Zhu, Z. Liu, J. Du, and W. L. Li, "Vibration behaviors of a box-type structure built up by plates and energy transmission through the structure," *Journal of Sound and Vibration*, vol. 331, no. 4, pp. 849–867, 2012.

[88] X. Lv, D. Shi, Q. Wang, and Q. Liang, "A unified solution for the in-plane vibration analysis of multi-span curved Timoshenko beams with general elastic boundary and coupling conditions," *Journal of Vibroengineering*, vol. 18, no. 2, pp. 1071–1087, 2016.

[89] F. Gruttmann and W. Wagner, "Shear correction factors in timoshenko's beam theory for arbitrary shaped cross-sections," *Computational Mechanics*, vol. 27, no. 3, pp. 199–207, 2001.

[90] Y. Zhou, Q. Wang, D. Shi, Q. Liang, and Z. Zhang, "Exact solutions for the free in-plane vibrations of rectangular plates with arbitrary boundary conditions," *International Journal of Mechanical Sciences*, vol. 130, pp. 1–10, 2017.

[91] V. Tajeddini and A. Ohadi, "Three-dimensional vibration analysis of functionally graded thick, annular plates with variable thickness via polynomial-Ritz method," *Journal of Vibration and Control*, vol. 18, no. 11, pp. 1698–1707, 2012.

[92] V. Tajeddini, A. Ohadi, and M. Sadighi, "Three-dimensional free vibration of variable thickness thick circular and annular isotropic and functionally graded plates on Pasternak foundation," *International Journal of Mechanical Sciences*, vol. 53, no. 4, pp. 300–308, 2011.